 doi:10.20944/preprints202002.0425.v1

Updated European hydraulic pedotransfer functions with communicated uncertainties in the predicted variables (euptfv2)

Brigitta Szabó[1], Melanie Weynants[2], Tobias KD Weber[3]

[1]Institute for Soil Sciences and Agricultural Chemistry, Centre for Agricultural Research, Herman Ottó út 15, 1022 Budapest, Hungary. ORCID: 0000-0003-1485-8908
[2]European Commission Joint Research Centre, via Enrico Fermi 2749, 21027 Ispra, Italy
[3]Institute of Soil Science and Land Evaluation, University of Hohenheim, Emil-Wolff-Straße 27, 70593 Stuttgart, Germany. ORCID: 0000-0002-3448-5208

Correspondence to: Brigitta Szabó (toth.brigitta@agrar.mta.hu)

Abstract. Soil hydraulic properties are often derived indirectly, i.e. computed from easily available soil properties with pedotransfer functions (PTFs), when those are needed for catchment, regional or continental scale applications. When predicted soil hydraulic parameters are used for the modelling of the state and flux of water in soils, uncertainty of the computed values can provide more detailed information when drawing conclusions. The aim of this study was to update the previously published European PTFs (Tóth et al., 2015, euptf v1.4.0) by providing prediction uncertainty calculation built into the transfer functions. The new set of algorithms was derived for point predictions of soil water content at saturation (0 cm matric potential head), field capacity (both -100 and -330 cm matric potential head), wilting point (-15.000 cm matric potential head), plant available water, and saturated hydraulic conductivity, as well as the Mualem-van Genuchten model parameters of the moisture retention and hydraulic conductivity curve. The minimum set of input properties for the prediction is soil depth and sand, silt and clay content. The effect of including additional information like soil organic carbon content, bulk density, calcium carbonate content, pH and cation exchange capacity were extensively analysed. The PTFs were derived adopting the random forest method. The advantage of the new PTFs is that they i) provide information about prediction uncertainty, ii) are significantly more accurate than the euptfv1, iii) can be applied for more predictor variable combinations than the euptfv1, 32 instead of 5, and iv) are now also derived for the prediction of water content at -100 cm matric potential head and plant available water content.

1 Introduction

Quantitative information on state and flux of water in the critical zone is important for a wide range of environmental process models and decision support systems related to land surface processes (Lin, 2010; Zhao et al., 2018). Performance of hydrologic, climate, crop and other models related to soil hydrological processes depends on the quality and resolution of soil hydraulic input parameters (Vereecken et al., 2015). Simulations of variably saturated moisture fluxes in the vadose zone either

Preprints (www.preprints.org) | NOT PEER-REVIEWED | Posted: 28 February 2020 doi:10.20944/preprints202002.0425.v1

rely on simple modelling approaches which only require few directly measureable input variables such as porosity, field capacity, and wilting point, or on the Richards equation. While the former are simple and straightforward to obtain, the Richards equation requires knowledge about the soil hydraulic properties over the full moisture range. In practice, one of the most common approaches to describe the water retention and hydraulic conductivity curves required to solve the Richards equation is arguably (Weber et al., 2019) the Mualem-van Genuchten model (MVG) (van Genuchten, 1980; Mualem, 1976). Since soil hydraulic measurements in the laboratory or in the field are often time consuming, expensive and difficult, indirect methods for estimating soil hydraulic properties using widely available surrogate data have been developed (Schaap, 2006). To date, a large number of pedotransfer functions have become popular to predict soil hydraulic properties and MVG model parameters (Van Looy et al., 2017).

Information on the uncertainty of the predicted soil hydraulic properties is important for modelling the state and flux of water in soil. The source of prediction uncertainty can be threefold: it can stem from the i) predictor (e.g. measurement uncertainty, non-representativeness of a sample), ii) predicted variables (e.g. uncertainty in the estimated soil hydraulic model parameters), and the iii) algorithm which describes the relation between the two. Information on the uncertainty of the predictor variables is commonly not available in PTFs derived before the 2000s, but has become a more intensively studied topic in the last decade. For example, Weynants *et al.* (2009) quantified uncertainty of derived PTFs related to experimental, model and fitting errors with the one-step inversion method. Deng et al. (2009) differentiated and quantified intrinsic and input uncertainty of PTFs. Román Dobarco *et al.* (2019) introduced prediction interval coverage probability to assess prediction uncertainty in PTFs derived on French soils. McNeill et al. (2018) provided estimation of the distribution and confidence intervals of the predicted soil hydraulic property (i.e. water content at 100 cm and 15000 cm matric potential head and total available water). In the field of soil mapping it is an even more extensively studied topic where different computational methods have been proposed to assess uncertainty of the mapped properties. Examples are estimation of the 90% prediction intervals based on a triangular distribution (Odgers *et al.* 2014), quantification of mapped soil properties uncertainties by quantile regression forest (Vaysse and Lagacherie, 2017), and a detailed comparison of uncertainties in mapped soil organic carbon content by different geostatistical and machine learning methods (Szatmári and Pásztor, 2019).

Machine learning methods can be more robust to construct PTFs in comparison to previous approaches such as linear regression or simple decision trees if relationship between the predictors and response is highly non-linear (Araya and Ghezzehei, 2019). The random forest algorithm (Breiman, 2001) is able to outperform other machine learning methods (Olson et al., 2018), which was also shown for predicting soil properties (Hengl et al., 2018; Nussbaum et al., 2018). Improvements in computing power, statistical methods and statistical software provide the possibility to apply more easily even complex models on large datasets. Therefore, complexity of a prediction algorithm is no longer a barrier in selecting a suitable algorithm to develop and apply PTFs. Most of the recent machine learning algorithms have the built in possibility to compute the uncertainty in the predicted variable, e.g. by quantile regression forest (Meinshausen, 2006) or generalized boosted regression (Ridgeway, 2017). If PTFs are derived with these algorithms, the uncertainty of the predicted soil property can be directly estimated when applying the PTF (Szabó et al., 2019a).

Despite the above mentioned developments, the euptfv1 (Tóth et al., 2015) and derived soil hydraulic property maps for Europe on a 1km and 250m grid (Tóth et al., 2017) do not include uncertainties in the prediction. Hence, the aim of our study was to update the euptfv1 by deriving a new set of soil hydraulic PTFs (euptfv2) providing uncertainty calculation built into the PTF model. For this, we rely heavily on the datasets used in the construction of the euptfv1. Methodologically, we constructed new soil hydraulic PTFs on the basis of the random forest method which facilitates a quantification of prediction uncertainties. The predicted variables of interest included soil water content at saturation, field capacity and wilting point, plant available water content, saturated hydraulic conductivity, MVG parameters of the moisture retention and hydraulic conductivity curves. The predictions are based on easily available soil properties. The predictor variables were similar to those of euptfv1, except the topsoil and subsoil distinction, which was replaced by mean soil depth of the sample, since it is typically known, anyway. Additionally, the improved performance of the euptfv2 was assessed against predictions using the earlier version. Moreover, we determined the minimum sufficient predictor variables for 32 input variables combinations.

2 Materials and Methods

The construction of a pedotransfer function requires three elements: predictor variables, predicted variables as the property of interest, and a transfer method between the former two. The predicted variables are in this case directly measured soil hydraulic properties on samples contained in a large pan-European dataset, ensuring a representativeness of the PTF for Europe. Additionally, Tóth et al. (2015) had fitted MVG model parameters for each sample dataset individually by inverse modelling, which we reused in this study.

2.1 Dataset

The European Hydropedological Data Inventory (EU-HYDI) (Weynants et al., 2013) provided the basis for the preparation of the prediction algorithms. The dataset partitions for training and testing the prediction algorithms were almost identical to the ones used in Tóth et al. (2015), except that the samples had to have information on soil depth as well. Depending on the soil hydraulic property of interest, 76-99% of the originally selected samples were used to derive the new PTFs. It enabled comparison of the performance between the EU-PTFs (Tóth et al., 2015) – built in the euptfv1 (Weynants and Tóth, 2014) – and their improved version (euptfv2). Table 1 shows the number of samples in the training and test sets.

2.2 Predicted soil hydraulic properties

Prediction algorithms were derived for each of the following soil hydraulic properties:

- water content at saturation (THS): water content at 0 cm matric potential head;
- water content at field capacity at
  - -100 cm matric potential head (FC_2), and
  - -330 cm matric potential head and (FC);

Preprints (www.preprints.org) | NOT PEER-REVIEWED | Posted: 28 February 2020 doi:10.20944/preprints202002.0425.v1

- water content at wilting point (WP): water content at -15000 cm matric potential head;
- plant available water content (AWC) based on the following equations:
  - $AWC = FC - WP$ (1)
  - $AWC\_2 = FC\_2 - WP$ (2)
- saturated hydraulic conductivity (KS): hydraulic conductivity at 0 cm matric potential head;
- Mualem-van Genuchten model parameters (VG; for the water retention model only, MVG; for the water retention and hydraulic conductivity model).

Transformation of predicted variables, and explanation on how (i) the water content at a certain matric potential head values were harmonized and (ii) the Mualem-van Genuchten model parameters were fitted is provided in great detail in (Tóth et al., 2015). FC_2 was not predicted in euptfv1 and was determined in this study as follows. In the EU-HYDI, 8231 samples have at least one water content observation in the matric potential head range -110 to -95 cm. 86% of those have a measured water retention value exactly at -100 cm matric potential head. In 10% of the cases, FC_2 was set to the water content measured at the closest matric potential head in the range [-110, -95]. In the absence of a measured value at -100 cm, in 4 % of the cases, FC_2 was computed by linear interpolation between the two closest matric potential heads smaller and greater than -100 cm. In the case of AWC and AWC_2 direct and indirect predictions were analysed, i.e. AWC was once predicted directly from the predictor variables and once computed from the PTF predicted variables WP, and FC and FC_2, respectively.

2.3 Predictor variables

As predictors we used the following easily available soil properties: the particle size densities (PSD) characterised by the mass-percentages of clay (<2 µm), silt (2–50 µm) and sand (50–2000 µm), organic carbon content (OC; mass-%) , bulk density (DB; g cm^{-3}), calcium carbonate content (CACO3; mass-%), pH in water (PH_H2O; -), cation exchange capacity (CEC; cmol (+) kg^{-1}), and replaced the former topsoil and subsoil distinction in euptfv1 with mean soil depth (cm) (DEPTH). At minimum, the predictor variables, clay, silt and sand content, as well as mean soil depth were used regardless of predicted variable. In addition to that, we tested every possible combination of the other above mentioned soil properties (predictor variables) to determine which combination significantly improves the performance of the predictions. A total of 32 different combinations of predictor variables were studied in their respective ability to predict the nine different properties of interest; i.e. the set of soil hydraulic properties and model parameters.

Replacing the topsoil/subsoil distinction with depth for the new PTFs was supported by the fact that this information is commonly available, too, or can be based on expert knowledge. Introducing more accurate information on depth might improve the performance without using machine learning algorithms for the prediction. However, we did not test this hypothesis, because our aim was to provide uncertainty of the predictions related to predictor variables of the PTFs. Tested predictor variables are shown in Table 1 with number of samples used to derive the PTFs and compute their performance.

Preprints (www.preprints.org) | NOT PEER-REVIEWED | Posted: 28 February 2020 doi:10.20944/preprints202002.0425.v1

2.4 The Random Forest algorithm to derive PTFs

We derived the PTFs adopting the random forest method (Breiman, 2001), implemented in the 'ranger' R package (Wright and Ziegler, 2017). We selected this method, because (i) it is among the best performing prediction algorithms if there is a complex interaction structure in the dataset (Boulesteix et al., 2012), (ii) it computes quantiles of the predicted values, (iii) parallel processing is supported which saves significant computation time, and (iv) the initially black-box type algorithm can be interpreted based on computing variable importance and analysing partial dependence plots implemented in the 'pdp' R package (Greenwell, 2017b).

In the case of a continuous response variable, a random forest is an ensemble of de-correlated regression trees (Breiman, 2001). The regression tree approach divides the predictor space into non-overlapping regions through minimizing the residual sum of squares. The aim of the method is to subset the data as homogeneously as possible at each split. The observations can be assigned to the defined regions in which the mean of the response variable is the predicted value. Single trees of the forest are noisy and limited in performance, but if many unbiased trees are derived and averaged with bagging, the variance is reduced and performance of the prediction improves (Hastie et al., 2009). Building of de-correlated trees is achieved by randomization at two levels. Firstly, each tree of the forest is grown on a randomly selected two thirds of the data with replacement, which is called bootstrap sample or in-bag fraction. Secondly, at each node of a single tree, randomly selected sets of predictors are analysed to split the data. This feature of randomization allows correlation between the response variables (Ziegler and König, 2014), which is an important advantage in the case of pedotransfer functions where predictors are often highly correlated.

Parameter tuning of the ranger was performed with the 'caret' R package (Kuhn et al., 2017, 2018). With the implemented train function, a fivefold cross-validation was repeated ten times to tune the number of randomly selected predictor variables at each split ($mtry$) and find the best performing splitting rule ($splitrule$) during training. We started the tuning by setting the number of randomly selected predictor variables to two, then added one by one until the number of all available predictors for each input variable combination was reached. All three built-in splitting rules in the ranger function were tuned, namely $variance$, $extratrees$ and $maxstat$. The minimum node size was kept to 10. In addition to the tuning options included in the train function of the caret package, we optimized the number of trees in the forest. The above described tuning was performed by discretely altering the number of trees in the forest in separate tuning steps to 50, 100, 200, 500 and 1000, analysing the results and choosing the best number of trees for the random forest.

We analysed the relevance of predictors and their influence on the response variable. The relevance of predictors was determined by computing the variable importance based on the mean decrease in impurity (Hastie et al., 2009) in the ranger function. The marginal effect of some selected predictors on the response – soil hydraulic parameters – was analysed with partial dependence plots (Greenwell, 2017a, 2017b).

The final prediction algorithm was built on the whole training set based on the result of the tuning. For the description of the uncertainty, quantile regression was performed. Quantiles of the predicted values were estimated as implemented in quantile

Preprints (www.preprints.org) | NOT PEER-REVIEWED | Posted: 28 February 2020 doi:10.20944/preprints202002.0425.v1

regression forest (Meinshausen, 2006). We analysed the 90% prediction interval for all predictions, but the derived algorithms (PTFs) provide the possibility to compute the individual predictions of each tree.

2.5 Evaluation of derived PTFs

The performance of the PTFs was calculated using the median values predicted by the random forests. It was described with the root mean square error (RMSE) (Eq. 3.), and the coefficient of determination (R^2) (Eq. 4.) computed for the training and test sets.

$$\boldsymbol{RMSE} = \sqrt{\frac{1}{N}\sum_{i=1}^{N}(\boldsymbol{y_i} - \boldsymbol{\hat{y}_i})^2} = \sqrt{\boldsymbol{MSE}} \tag{3}$$

$$\boldsymbol{R^2} = \boldsymbol{1} - \frac{\sum_{i=1}^{N}(y_i - \hat{y}_i)^2}{\sum_{i=1}^{N}(y_i - \bar{y})^2} \tag{4}$$

where y_i is the measured and $\hat{y}_i$ the predicted soil water content or log-transformed saturated or unsaturated hydraulic conductivity, $\bar{y}_i$ is the average of y_i, N is the number of y_i and $\hat{y}_i$ data pairs, and MSE is the mean square error.

For each predicted variable, there was an initial set of 32 predictor combinations (Table 1), whose individual performance for each of the predicted variables was assessed. Based on the test results, we derived recommendations which PTF should be used when certain sets of predictor variables are available. We compared the performance of PTFs to quantify if there are significant differences between the predictions as a consequence of adding certain soil properties to the predictor variables. We also compared the performance of point and parameter estimations for those input combinations, which reflect the most frequently available soil property combination from a practical point of view.

Additionally, the performance of the presented random forest based PTFs was compared to that of the euptfv1 (Tóth et al., 2015). For comparison, those PTFs from euptfv2 were selected which corresponded to the analysed input variable combination of the euptfv1.

The comparison of PTFs was done using a non-parametric Kruskal-Wallis test at the 5% significance level applied on the MSE values – computed on TEST_BASIC and/or TEST_CHEM+ sets (Table 1) – using the R package agricolae (De Mendiburu, 2017). Recommendation of PTFs for a given set of predictor variables was based on the performance of euptfv2 on the test sets. If there was no significant difference in performance, the PTF derived from the largest population was selected.

All statistical analysis was performed in R [version 3.6.0] (R Core Team, 2019).

3 Results and discussion

3.1 General performance

In the process of tuning the random forest parameters, the number of trees was found to be sufficient when set to 200 in all cases. The number of candidate predictors was found to be higher than the recommended square root of the number of available predictor variables (p) in most of the cases, especially when p was greater than 5 (Fig.1). When optimizing the splitting rules

to build the trees in the forest, overall, the best performance was achieved by the *extratrees* rule in 54 %, by the *variance* rule in 28%, and by the *maxstat* rule in 18% of the cases (Fig. 1).

The RMSE values were between 0.020 and 0.068 cm^3 cm^{-3} for THS (Table 2), 0.046 and 0.055 cm^3 cm^{-3} for FC (Table 3), 0.040 and 0.060 cm^3 cm^{-3} for FC_2 (Table 4), 0.037 and 0.048 cm^3 cm^{-3} for WP (Table 5), 0.043 and 0.053 cm^3 cm^{-3} for AWC (Table S1), 0.045 and 0.060 cm^3 cm^{-3} for AWC_2 (Table S2), and 0.089 and 1.18 $\log_{10}$ (cm day^{-1}) for KS (Table 6) in the case of including different predictor variables computed on the test sets. In the case of VG and MVG, RMSE for the entire matric potential head range was between 0.041 and 0.068 cm^3 cm^{-3} for the moisture retention (Table 7) and 0.61 and 0.71 $\log_{10}$ (cm day^{-1}) for the hydraulic conductivity (Table 8). These RMSE values are within the range of recently published PTFs (McNeill et al., 2018; Nguyen et al., 2017; Román Dobarco et al., 2019; Zhang and Schaap, 2017). In the case of the point estimations, Figures 2, S1 depict the scatterplots of measured and predicted soil hydraulic parameters with 90% prediction interval. Performance of the worst to best PTFs are shown. The addition of predictors that significantly improve the predictions also decreases the uncertainty. Figures S2, S4, S6, S8, S10, S12, S14, S16, S19 show the squared error of the derived PTFs computed on the TEST_BASIC and TEST_CHEM+ sets. The PTFs are ordered based on their performance. Density plots of measured and predicted soil hydraulic values are included in Figures S3, S5, S7, S9, S11, S13, S15, S17, S20. Plots show the PTFs that use the most frequently available predictors.

This study strengthens the importance of chemical soil properties in the prediction. CEC was found to be an important predictor by Pachepsky and Rawls (1999) for FC and WP, by Botula et al. (2013) for water retention at several matric potential head values, and by Hodnett and Tomasella (2002) for the VG parameters. Hodnett and Tomasella (2002) showed that pH influenced all four VG parameters. The role of CACO3 was shown to be not significant in the study of (Khodaverdiloo et al., 2011). They highlight that a possible influence of CACO3 might already have been indirectly included by bulk density. The role of PSD, BD and OC has been studied extensively by various authors, e.g. Nemes et al. (2003); Rawls et al. (2003); Vereecken et al. (1989); Weynants et al. (2009); Wösten et al. (1999), which is in line with the general pattern of variable influence we see in this study.

Table S3 summarizes the recommended PTF for each combination of available predictor variables. The importance and influence of soil properties on the performance of hydraulic PTFs and results of partial dependence plots are reported below by predicted soil hydraulic properties.

3.2 Point estimations

The performance of the PTFs was computed for the training and test sets (Tables 2-8 and Tables S1-2) indicating the presence of significant differences. For each predictor variable, the recommended PTF number is indicated and its predictor variables are highlighted in bold font in the respective tables. For easier comparison with euptfv1, the corresponding PTF number used in Tóth et al. (2015) is additionally provided in each table. In the following, detailed results of the constructed PTFs for the individual predicted variables are presented and discussed.

Preprints (www.preprints.org) | NOT PEER-REVIEWED | Posted: 28 February 2020 doi:10.20944/preprints202002.0425.v1

Water content at saturation

Table 2, Figures S2 and S3 show the performance of the PTFs predicting THS. The best performing random forest is PTF03. It is also the one trained on the largest population. It uses PSD, DEPTH and BD as predictors. For the prediction of THS, the most important variable by far is BD (Fig. 3). When BD is not used for the computation of THS, values above 0.60 $cm^3\ cm^{-3}$ are not well predicted (Fig. S3). The addition of OC or CACO3 or PH_H2O to PSD and DEPTH improves significantly the performance of the PTF. The picture changes if BD is known: if PSD, DEPTH and BD were available, further addition of OC or CACO3 or PH_H2O or CEC does not significantly improve the prediction, neither do their combinations. Figure 4 shows the dependence of THS on OC and BD, considering the average effect of the other predictor variables – i.e. PSD and DEPTH. When BD is lower than 1.5 g cm^{-3} changes in OC does not influence THS. If BD is larger than 1.5 g cm^{-3}, samples with higher OC have higher THS.

Water content at field capacity

The performance of the PTFs computed on training and test set are shown in Table 3, Figures S4 and S5 for FC_2 and in Table 4, Figures S6 and S7 for FC. The best performing PTF derived from the largest population is the one using i) PSD, DEPTH, OC, BD and PH_H2O (PTF18) in the case of FC_2, and ii) PSD, DEPTH, OC and BD (PTF07) for FC.

For FC_2, the two most important variables are USSAND and BD (Fig. 3). When BD and USSAND increase, FC_2 decreases (Fig. 4). Adding OC or BD to PSD and DEPTH significantly improves the prediction of FC_2. If either of CACO3, PH_H2O or CEC is added as a further predictor to PSD and DEPTH, the performance of the PTF does not significantly improve. If PSD, DEPTH and BD are available, adding OC or CACO3 or PH_H2O does not significantly improve the prediction. Including CEC as an additional predictor besides PSD, DEPTH and BD, significantly improves the estimation of FC_2.

USSAND and USCLAY are the two most important variables for the prediction of FC (Fig. 3). Instead of analysing these two soil properties, both characterizing the soil texture, we include OC next to USSAND in the partial dependence plot analysis, because the amount of OC can be altered due to change in climate, land use, soil and water management, cropping systems, etc. (Wiesmeier et al., 2019). Within the range of OC in the dataset FC increases with increasing OC regardless of USSAND content by up to 0.08 $cm^3\ cm^{-3}$ even when USSAND is greater than 60 % (Fig. 4). Adding OC or CEC to PSD and DEPTH significantly improves prediction of FC. The effect of CEC on the prediction of FC was also shown by Pachepsky and Rawls (1999). BD or CaCO3 or PH_H2O do not significantly improve the predictions if PSD, DEPTH, or PSD, DEPTH and OC are available. Predictions significantly improve when both CaCO3 and PH_H2O are added as predictors to PSD, DEPTH and OC.

Water content at wilting point

The performance of PTFs derived for WP prediction is shown in Table 5, Figures S8 and S9. Among the best performing PTFs, PTF09 is derived on the largest training set. It uses PSD, DEPTH, OC and PH_H2O as predictors. Even though the most important variables for WP prediction were USCLAY and USSAND (Fig. 3), we included OC on the partial dependence plot

(Fig. 4) as in the FC analysis. USCLAY had the strongest influence on WP. The influence of OC on WP can be detected for soils with OC less than 4 % and USCLAY less than 50 %. Below 10 % USCLAY, the WP slightly increases with increasing OC. When USCLAY is between 10 and 50 % and OC is less than 4%, increasing OC generally decreases WP.

OC significantly improves the prediction of WP if added to PSD and DEPTH. If BD or CACO3 or PH_H2O or CEC are added to PSD and DEPTH, the performance of the prediction does not improve significantly. Adding CACO3 and CEC to PSD, DEPTH and OC significantly improves the prediction.

Plant available water content

Table S1, S2 and Figures S1, S10-13 show the performance of AWC and AWC_2 predictions. PTF03 is the best performing algorithm with largest training set for both. It considers PSD, DEPTH and BD for the prediction. For both AWC and AWC_2, BD is the most important predictor among the analysed variables (Fig. 3). The second most important variable is USCLAY in the case of AWC_2 and USSILT for AWC. Increasing BD and USCLAY decreases AWC_2. In the case of AWC, increasing BD and decreasing USSILT decreases the water content (Fig. 4).

OC and BD significantly improve the prediction of AWC_2 when added as input variables next to PSD and DEPTH. If either BD or OC is already included, adding the respective other, does not significantly improve the prediction. Neither PH_H2O, CACO3 nor CEC significantly improve the prediction.

For the prediction of AWC, further addition of only BD or OC or CACO3 or PH_H2O or CEC to PSD and DEPTH does not significantly improve the prediction. If both OC and BD are included as predictors next to PSD and DEPTH, the prediction significantly improves.

There is no significant difference between direct and indirect predictions, neither for AWC nor for AWC_2. However, the size of the test set used for the statistical analysis is limited. There were only 145 samples in the TEST_BASIC set and 64 samples in TEST_CHEM+ set after merging datasets available for both direct and indirect predictions for analysing AWC, and 70 and 34 samples in the case of AWC_2. Thus, if prediction of FC_2/FC and WP are needed in addition to AWC_2/AWC, we recommend to compute AWC from those to save on computing time. Variation in AWC could be explained less efficiently (Table S1, S2) than the other studied water retention values but the performance of the prediction is comparable with that of published in the literature (Li et al., 2016; Malone et al., 2009).

Saturated hydraulic conductivity

The performance of KS prediction is shown in Table 6, Figure S14 and S15. The predictors of the best performing PTF derived on largest training set are PSD, DEPTH and OC (PTF02). The prediction of KS significantly improves if OC is included among the predictor variables next to PSD and DEPTH. No other predictors significantly improve the performance of the PTF. On the training dataset, when OC is greater than 2.5 %, the influence of clay content on KS is more dominant than that of OC (Fig. 4). In the case of KS prediction, the simplest best performing PTF has an RMSE of 0.94 $\log_{10}$(cm day^{-1}). PSD and CEC are the most important input variables for the prediction of KS when all nine variables are considered as predictors (Fig. 3). In

that case, OC is the fifth and BD is only the eighth most important variable. The prediction performance is influenced by the heterogeneity of measurement methods of KS in the EU-HYDI dataset. When the methods are homogeneous, the RMSE value is usually around 0.6-0.7 $\log_{10}$ (cm day^{-1}) (Zhang and Schaap, 2017). Araya and Ghezzehei (2019) report that the PTF with the highest accuracy in the literature has and RMSE of 0.3-0.4 $\log_{10}$ (cm day^{-1}). In Lilly et al. (2008), the performance of the KS predictions and findings were similar to this study. They report an RMSE between 0.95 and 1.09 $\log_{10}$(cm day^{-1}) for the KS prediction analysed with several input combinations. Even when information on soil structure and crack orientation was considered – next to topsoil and subsoil distinction, PSD, BD and OC – the RMSE was 0.97 $\log_{10}$(cm day^{-1}). BD would be among the most important variables, but also in their analysis its influence was masked out. They derived the PTFs on the HYPRES dataset (Wösten et al., 1999), which also includes very diverse methods to determine the saturated hydraulic conductivity and part of which is also contained in the EU-HYDI. The uncertainty in the predictions (Fig. 2) could be decreased if the predictions would be differentiated according to the measurement methods, but that might decrease the applicability of the PTFs. On the contrary, this study indicates the necessity to include saturated hydraulic conductivity values determined from many different measurement techniques, otherwise the PTFs are expected to lose their generality.

3.3 Parameter estimations

The performance of parametric PTFs are shown in Tables 7 and 8 and Figures 5, 6, S16-S21. Figure 7 illustrates the importance of variables for the prediction of VG and MVG parameters. The best performing PTF derived on the largest training set is PTF29 – with PSD, DEPTH, OC, BD, PH_H2O and CEC – for MRC and PTF27 – with PSD, DEPTH, OC, BD, CACO3, PH_H2O – for HCC.

For θ_r, overall, BD is the most important predictor while all other predictors show similar variable importance (Fig. 7). Interpretation of this parameter is complex, but it was demonstrated that it is influenced by the soil specific surface area (Assouline and Or, 2013), and the measured data range (Weber et al. 2019). For θ_s, the most important predictor is by far BD, similarly to THS. The importance of CEC has to be noted for the prediction of parameters α, n and L. For prediction of parameter n – which relates to the pore size distribution – USCLAY and USSAND are the most important variables. K_0 is influenced by several soil properties besides those included in the dataset used here, e.g. pore connectivity, tortuosity, primary pore orientation, some of which are not direction. These properties cannot be directly inferred from other soil properties limiting the explanatory power of the available properties. The prediction of K_0 remains complex and challenging. Variable importance of all studied predictors is greater than 70%. Moreover, K_0 is influenced by the data quality, and; moreover, is correlated in parameter space, which is not treated, here.

Only a few studies have analysed the importance of CEC for MRC and HCC PTFs (Botula et al., 2013; Hodnett and Tomasella, 2002; Pachepsky and Rawls, 1999) which might be linked to the fact that CEC is rarely available in soil hydraulic datasets. It is noteworthy to highlight that all best performing MRC PTFs (PTF24, PTF28, PTF29, PTF30, PTF31) include CEC among the predictors (Table 7). In addition to that, Hodnett and Tomasella (2002) found that CEC was important for the prediction of

θ_r and α parameters of the van Genuchten model. This is because CEC provides indirect information on soil mineralogy and reflects soil specific surface area, charge density and pore size which influence soil water retention (Lal and Shukla, 2004).

Moisture retention curve

If BD or OC or CACO3 or CEC or PH_H2O are added as a predictor to information on PSD and DEPTH, the performance of the PTF significantly improves (Table 7., Fig. S16). Adding BD next to PSD and DEPTH improves the predictions more than adding OC (Table 7., Fig. S17). BD and OC together significantly improve the prediction compared to using PSD, DEPTH together with either BD or OC. Adding OC next to PSD, DEPTH, BD and chemical soil properties (CACO3 and/or CEC and /or PH_H2O) does not significantly improve the prediction. If PSD, DEPTH, CACO3 and CEC are available, further addition of PH_H2O does not improve the prediction. The best performing PTF includes USSAND, USSILT, USCLAY, DEPTH, BD, CACO3, CEC. Figure 5 shows a scatterplot of measured and predicted water content values, including the performance of the worst and the best performing PTF (PTF01 and PTF29). The importance of including chemical properties and most importantly bulk density among the predictors is visible when measured water contents are greater than 0.50 cm^3 cm^{-3}. Those high water content values are characteristic when the soil is close to saturation, thus indirect information about the structure is needed for more accurate predictions of those water content values. Parametric PTFs underestimate water content near saturation and between -200 and -15000 cm matric potential head (Fig. S18). Overestimation occurs between -10 and -50 cm matric potential head and above 16000 cm matric potential head. When chemical soil properties are included, the degree of underestimation decreases between -200 and -15000 cm matric potential head, but overestimation increases between -5 and -10 cm with around 0.02 cm^3 cm^{-3}.

Hydraulic conductivity curve

OC, CACO3, PH_H2O and CEC significantly improve the prediction of HCC when added to PSD and DEPTH. Adding BD next to PSD and DEPTH does not improve the predictions (Table 8, Fig. S19, S20). If PSD, DEPTH and OC are used as predictors, further addition of BD or CACO3 or PH_H2O or CEC does not significantly improve the performance of the PTFs. However, adding CaCO3 and CEC or PH_H2O significantly improve the prediction. The performance of the worst and the best performing PTF is shown on Figure 6. The PTF with only PSD and DEPTH underestimate hydraulic conductivity values smaller than 0.01 cm day^{-1}. When OC, BD, PH_H2O and CEC are included, the underestimation decreases. This could be explained by the fact that these predictors contain indirect information of soil particle surface area and surface characteristics, which are some of the governing properties of low hydraulic conductivities.

When soil chemical properties are not used as predictors, hydraulic conductivity is underestimated close to saturation and at matric potential heads smaller than -500 cm; overestimation occurs between -10 and -500 cm matric potential head (Fig. S21). If chemical properties are also considered, hydraulic conductivity is i) underestimated at matric potential head smaller than -5000 cm, and ii) overestimated between -5 and -5000 cm. With added information on chemical properties, the degree of underprediction decreases close to saturation and at the very dry end of the hydraulic conductivity curve. In parts, this is not

an effect of the PTFs but the limitations inherent to MVG to describe the entire hydraulic conductivity curve (Weber et al., 2019). Increase in prediction performance for values lower than 0.1 cm day^{-1} is visible also on Figure 6.

3.4 Comparison of point and parameter predictions

We compare the performance of the best point prediction methods (Table 2-5) with the best parameter estimations (Table 7) on the test sets. In 5 out of 20 cases, point predictions are significantly more accurate. In all other cases, we have no significant difference between point and parametric PTFs (Table 9). We found similar results in the case of euptfv1 (Tóth et al., 2015). Tomasella et al. (2003) and Børgesen and Schaap (2005) had comparable findings regarding the performance of point and parametric PTFs. We recommend to compute THS, FC, FC_2 and WP with the point PTFs, more detailed explanation on it is included in Tóth et al. (2015).

3.5 Comparison of euptfv1 and v2

In 14 out of 19 cases, the PTFs of euptfv2 perform significantly better predicting the test sets than the PTFs of euptfv1. In the remaining 5 cases there is no significant difference (Table 10). Predictions of FC and MRC improve in all cases. For THS, WP, and MVG only those PTFs did not improve significantly, for which comparisons on the TEST_CHEM+ set was possible – which includes reduced number of samples. The improvement of the PTFs is twofold, it is due to i) using random forest instead of single regression tree or linear regression and ii) including more detailed information on soil sampling depth, not only distinguishing topsoils and subsoils.

We recommend the use of euptfv2 instead of euptfv1 if continuous soil properties are available. If only texture classes – i.e. no particle size distribution – are available, class PTFs of euptfv1 can be used, that is PTF18 for modified FAO texture classes and PTF19 for USDA texture classes.

4 Conclusions

The updated EU-PTFs – euptfv2 – perform significantly better than euptfv1 and are applicable for 32 predictor variables combinations. Uncertainties of the predicted soil hydraulic properties and model parameters can be computed. These uncertainties are, without further discrimination, related to the considered input data, predictors and the applied algorithm. The euptfv2 includes transfer functions to compute soil water content at saturation (0 cm matric potential head), field capacity (both -100 and -330 cm matric potential head) and wilting point (-15.000 cm matric potential head), plant available water content computed with field capacity at -100 and -330 cm matric potential head, saturated hydraulic conductivity, and Mualem-van Genuchten parameters of the moisture retention and hydraulic conductivity curves. For analyses of the impact as well as the significance of the uncertainties on the predicted soil hydraulic properties and model parameters, further studies are required.

Code and data availability. The derived prediction algorithms (PTFs) are freely available for use built in a user friendly web interface from the Institute for Soil Sciences and Agricultural Chemistry Centre for Agricultural Research (https://ptfinterface.rissac.hu/, last access: 03 Feb 2020, Szabó et al., 2019b). An open source R software package was developed (Weber and Szabó, 2019) to assist the implementation of PTFs presented in this article and can be accessed at the European Soil Data Centre (http://eusoils.jrc.ec.europa.eu/). The PTFs – in RData format – and the R scripts used to derive them can be freely accessed from a public GitHub repository (https://github.com/TothSzaboBrigitta/euptfv2).

Supplement. The Supplement related to this article is available online.

Author contribution. BSZ, TKDW and MW conceptualized the study and designed the methodology. BSZ supervised the research. MW cured the EU-HYDI dataset. BSZ, TKDW and MW prepared scripts for the statistical analysis, BSZ carried out the formal analysis, visualization and coordinated building of the PTF web interface. BSZ and TKDW performed the validation. BSZ and TKDW wrote the paper with considerable input from MW.

Competing interests. The authors declare that they have no conflict of interest.

Acknowledgements. B. Szabó is supported by the Hungarian National Research, Development and Innovation Office (NRDI) under grant KH124765 and the János Bolyai Research Scholarship of the Hungarian Academy of Sciences. On behalf of János Bolyai Research Scholarship we thank for the usage of MTA Cloud (https://cloud.mta.hu/) that significantly helped us achieving the results published in this paper. We praise the individual scientists and their institutions in Europe who contributed in the establishment of the EU-HYDI database. We would like to thank Gergely Tóth and Luca Montanarella for their effort in coordinating the formation of the EU-HYDI database. T. K.D Weber's contribution was supported by the Collaborative Research Center 1253 CAMPOS (Project 7: Stochastic Modelling Framework), funded by the German Research Foundation (DFG, Grant Agreement SFB 1253/1 2017). We thank to Jeromos Rózsa for defining the computing infrastructure. We also thank to Dávid Gyurkó for building the web interface for the prediction algorithms.

References

Araya, S. N. and Ghezzehei, T. A.: Using Machine Learning for Prediction of Saturated Hydraulic Conductivity and Its Sensitivity to Soil Structural Perturbations, Water Resour. Res., 55(7), 5715–5737, doi:10.1029/2018WR024357, 2019.

Assouline, S. and Or, D.: Conceptual and Parametric Representation of Soil Hydraulic Properties: A Review, Vadose Zo. J., 12(4), doi:10.2136/vzj2013.07.0121, 2013.

Børgesen, C. D. and Schaap, M. G.: Point and parameter pedotransfer functions for water retention predictions for Danish

soils, Geoderma, 127(1–2), 154–167, doi:10.1016/j.geoderma.2004.11.025, 2005.

Botula, Y.-D., Nemes, A., Mafuka, P., Van Ranst, E. and Cornelis, W. M.: Prediction of Water Retention of Soils from the Humid Tropics by the Nonparametric -Nearest Neighbor Approach, Vadose Zo. J., 12(2), 1-17., doi:10.2136/vzj2012.0123, 2013.

Boulesteix, A. L., Janitza, S., Kruppa, J. and König, I. R.: Overview of random forest methodology and practical guidance with emphasis on computational biology and bioinformatics, Wiley Interdiscip. Rev. Data Min. Knowl. Discov., 2(6), 493–507, doi:10.1002/widm.1072, 2012.

Breiman, L.: Random Forests, Mach. Learn., 45, 5–32, 2001.

Deng, H., Ye, M., Schaap, M. G. and Khaleel, R.: Quantification of uncertainty in pedotransfer function-based parameter estimation for unsaturated flow modeling, Water Resour. Res., 45(4), doi:10.1029/2008WR007477, 2009.

van Genuchten, M. T.: A closed-form equation for predicting the hydraulic conductivity of unsaturated soils, Soil Sci. Soc. Am. J., 44, 892–898, 1980.

Greenwell, B.: Partial Dependence Plots, 15 [online] Available from: https://cran.r-project.org/web/packages/pdp/pdp.pdf%0Ahttps://github.com/bgreenwell/pdp, 2017a.

Greenwell, B. M.: pdp: An R Package for Constructing Partial Dependence Plots, R J., 9(1), 421–436 [online] Available from: https://journal.r-project.org/archive/2017/RJ-2017-016/RJ-2017-016.pdf, 2017b.

Hastie, T., Tibshirani, R. and Friedman, J.: The Elements of Statistical Learning. Data Mining, Inference, and Prediction., Second edi., Springer. [online] Available from: https://web.stanford.edu/~hastie/ElemStatLearn//printings/ESLII_print10.pdf (Accessed 19 November 2018), 2009.

Hengl, T., Nussbaum, M., Wright, M. N. and Heuvelink, B. M.: Random Forest as a Generic Framework for Predictive Modeling of Spatial and Spatio-temporal Variables, PeerJ Prepr., 6:e5518, doi:10.7287/peerj.preprints.26693v3, 2018.

Hodnett, M. G. and Tomasella, J.: Marked differences between van Genuchten soil water-retention parameters for temperate and tropical soils: a new water-retention pedo-transfer functions developed for tropical soils, Geoderma, 108(3–4), 155–180, doi:10.1016/S0016-7061(02)00105-2, 2002.

Khodaverdiloo, H., Homaee, M., van Genuchten, M. T. and Dashtaki, S. G.: Deriving and validating pedotransfer functions for some calcareous soils, J. Hydrol., 399(1–2), 93–99, doi:10.1016/j.jhydrol.2010.12.040, 2011.

Kuhn, M., Wing, J., Weston, S., Williams, A., Keefer, C., Engelhardt, A., Cooper, T., Mayer, Z., Benesty, M., Lescarbeau, R., Ziem, A., Scrucca, L., Tang, Y., Candan, C. and Hunt, T.: Package "caret" Classification and Regression Training Description Misc functions for training and plotting classification and regression models. [online] Available from: https://cran.r-project.org/web/packages/caret/caret.pdf, 2017.

Kuhn, M., Wing, J., Weston, S., Keefer, C., Engelhardt, A., Cooper, T., Mayer, Z., Kenkel, B., Team, R. C., Benesty, M., Lescarbeau, R., Ziem, A., Scrucca, L., Tang, Y., Candan, C. and Hunt, T.: caret: Classification and Regression Training. R package version 6.0-79. [online] Available from: https://github.com/topepo/caret/, 2018.

Lal, R. and Shukla, M. K.: Principles of soil physics, Marcel Dekker, Inc., New York., 2004.

Li, D., Gao, G. and Fu, B.: Predicting available water of soil from particle-size distribution and bulk density in an oasis – desert transect in northwestern China, J. Hydrol., 538, 539–550, doi:10.1016/j.jhydrol.2016.04.046, 2016.

Lilly, A., Nemes, A., Rawls, W. J. and Pachepsky, Y. a: Probabilistic approach to the identification of input variables to estimate hydraulic conductivity, Soil Sci. Soc. Am. J., 72(1), 16–24, doi:10.2136/sssaj2006.0391, 2008.

Lin, H.: Earth ' s Critical Zone and hydropedology : concepts , characteristics , and advances, Hydrol. Earth Syst. Sci., 14., 25–45, doi:10.5194/hess-14-25-2010, 2010.

Van Looy, K., Bouma, J., Herbst, M., Koestel, J., Minasny, B., Mishra, U., Montzka, C., Nemes, A., Pachepsky, Y. A., Padarian, J., Schaap, M. G., Tóth, B., Verhoef, A., Vanderborght, J., van der Ploeg, M. J., Weihermüller, L., Zacharias, S., Zhang, Y. and Vereecken, H.: Pedotransfer Functions in Earth System Science: Challenges and Perspectives, Rev. Geophys., 55(4), 1199–1256, doi:10.1002/2017RG000581, 2017.

Malone, B. P., McBratney, A. B., Minasny, B. and Laslett, G. M.: Mapping continuous depth functions of soil carbon storage and available water capacity, Geoderma, 154(1–2), 138–152, doi:10.1016/j.geoderma.2009.10.007, 2009.

McNeill, S. J., Lilburne, L. R., Carrick, S., Webb, T. H. and Cuthill, T.: Pedotransfer functions for the soil water characteristics of New Zealand soils using S-map information, Geoderma, 326(April), 96–110, doi:10.1016/j.geoderma.2018.04.011, 2018.

Meinshausen, N.: Quantile Regression Forests, J. Mach. Learn. Res., 7, 983–999, 2006.

De Mendiburu, F.: agricolae: Statistical Procedures for Agricultural Research. R package version 1.2-8. [online] Available from: https://cran.r-project.org/package=agricolae, 2017.

Mualem, Y.: A new model for predicting the hydraulic conductivity of unsaturated porous media., Water Resour. Res., 12(3), 513–522, 1976.

Nemes, A., Schaap, M. and Wösten, J.: Functional evaluation of pedotransfer functions derived from different scales of data collection, Soil Sci. Soc. Am., 67, 1093–1102 [online] Available from: https://www.soils.org/publications/sssaj/abstracts/67/4/1093 (Accessed 29 April 2013), 2003.

Nguyen, P. M., Haghverdi, A., Pue, J. De, Botula, Y., Le, K. V, Waegeman, W. and Cornelis, W. M.: Comparison of statistical regression and data-mining techniques in estimating soil water retention of tropical delta soils, Biosyst. Eng., 153, 12–27, doi:10.1016/j.biosystemseng.2016.10.013, 2017.

Nussbaum, M., Spiess, K., Baltensweiler, A., Grob, U., Keller, A., Greiner, L., Schaepman, M. E. and Papritz, A.: Evaluation of digital soil mapping approaches with large sets of environmental covariates, SOIL, 4, 1–22, doi:10.5194/soil-4-1-2018, 2018.

Odgers, N. P., McBratney, A. B. and Minasny, B.: Digital soil property mapping and uncertainty estimation using soil class probability rasters, Geoderma, 237, 190–198, doi:10.1016/j.geoderma.2014.09.009, 2014.

Olson, R. S., La Cava, W., Mustahsan, Z., Varik, A. and Moore, J. H.: Data-driven advice for applying machine learning to bioinformatics problems, in Biocomputing 2018, edited by R. B. Altman, A. K. Dunker, L. Hunter, M. D. Ritchie, T. A. Murray, and T. E. Klein, pp. 192–203, World Scientific., 2018.

Pachepsky, Y. A. and Rawls, W. J.: Accuracy and Reliability of Pedotransfer Functions as Affected by Grouping Soils, Soil Sci. Soc. Am. J., 63(6), 1748–1757, doi:10.2136/sssaj1999.6361748x, 1999.

R Core Team: R: A language and environment for statistical computing., [online] Available from: https://www.r-project.org, 2019.

Rawls, W., Pachepsky, Y. and Ritchie, J.: Effect of soil organic carbon on soil water retention, Geoderma, 116(1–2), 61–76, doi:10.1016/S0016-7061(03)00094-6, 2003.

Ridgeway, G.: gbm: Generalized Boosted Regression Models. R package version 2.1.3., 2017.

Román Dobarco, M., Cousin, I., Le Bas, C. and Martin, M. P.: Pedotransfer functions for predicting available water capacity in French soils, their applicability domain and associated uncertainty, Geoderma, 336(April 2018), 81–95, doi:10.1016/J.GEODERMA.2018.08.022, 2019.

Schaap, M. G.: Models for Indirect Estimation of Soil Hydraulic Properties, in Encyclopedia of Hydrological Sciences, edited by M. G. Anderson and J. J. McDonnell, John Wiley & Sons, Ltd, Chichester, UK., 2006.

Szabó, B., Szatmári, G., Takács, K., Laborczi, A., Makó, A., Rajkai, K. and Pásztor, L.: Mapping soil hydraulic properties using random-forest-based pedotransfer functions and geostatistics, Hydrol. Earth Syst. Sci., 23, 2615–2635, doi:10.5194/hess-23-2615-2019, 2019a.

Szabó, B., Gyurkó, D., Weynants, M. and Weber, T. K. D.: Web interface for European hydraulic pedotransfer functions (euptfv2), [online] Available from: https://ptfinterface.rissac.hu/, 2019b.

Szatmári, G. and Pásztor, L.: Comparison of various uncertainty modelling approaches based on geostatistics and machine learning algorithms, Geoderma, 337(August 2018), 1329–1340, doi:10.1016/j.geoderma.2018.09.008, 2019.

Tomasella, J., Crestana, S. and Rawls, W. J.: Comparison of Two Techniques to Develop Pedotransfer Functions for Water Retention, Soil Sci. Soc. Am. J., 67, 1085–1092, 2003.

Tóth, B., Weynants, M., Nemes, A., Makó, A., Bilas, G. and Tóth, G.: New generation of hydraulic pedotransfer functions for Europe., Eur. J. Soil Sci., 66(1), 226–238, doi:10.1111/ejss.12192, 2015.

Tóth, B., Weynants, M., Pásztor, L. and Hengl, T.: 3D soil hydraulic database of Europe at 250 m resolution, Hydrol. Process., 31(14), 2662–2666, doi:10.1002/hyp.11203, 2017.

Vaysse, K. and Lagacherie, P.: Using quantile regression forest to estimate uncertainty of digital soil mapping products, Geoderma, 291, 55–64, doi:10.1016/j.geoderma.2016.12.017, 2017.

Vereecken, H., Maes, J., Feyen, J. and Darius, P.: Estimating the Soil Moisture Retention Characteristic From Texture, Bulk Density, and Carbon Content, Soil Sci., 148(6), 389–403, doi:10.1097/00010694-198912000-00001, 1989.

Vereecken, H., Huisman, J. A., Franssen Hendricks, H. J., Brüggemann, N., Bogena, H. R., Kollet, S., Javaux, M., van der Kruk, J. and Vanderborght, J.: Soil hydrology: Recent methodological advances, challenges, and perspectives, Water Resour. Res., 51, 1–18, doi:10.1002/2014WR016852.Received, 2015.

Weber, T. K. D. and Szabó, B.: euptf2lite: Prediction of van Genuchten-Mualem model parameters. R package version 0.1.3., 2019.

Weber, T. K. D., Durner, W., Streck, T. and Diamantopoulos, E.: A Modular Framework for Modeling Unsaturated Soil Hydraulic Properties Over the Full Moisture Range, Water Resour. Res., 4994–5011, doi:10.1029/2018WR024584, 2019.

Weynants, M. and Tóth, B.: The euptf package., Eur. Soil Portal., 5 [online] Available from: https://esdac.jrc.ec.europa.eu (Accessed 19 May 2019), 2014.

Weynants, M., Vereecken, H. and Javaux, M.: Revisiting Vereecken Pedotransfer Functions: Introducing a Closed-Form Hydraulic Model, Vadose Zo. J., 8(1), 86, doi:10.2136/vzj2008.0062, 2009.

Weynants, M., Montanarella, L., Tóth, G., Arnoldussen, A., Anaya Romero, M., Bilas, G., Borresen, T., Cornelis, W., Daroussin, J., Gonçalves, M. D. C., Haugen, L.-E., Hennings, V., Houskova, B., Iovino, M., Javaux, M., Keay, C. A., Kätterer, T., Kvaerno, S., Laktinova, T., Lamorski, K., Lilly, A., Mako, A., Matula, S., Morari, F., Nemes, A., Patyka, N. V., Romano, N., Schindler, U., Shein, E., Slawinski, C., Strauss, P., Tóth, B. and Woesten, H.: European HYdropedological Data Inventory (EU-HYDI), EUR – Scientific and Technical Research series – ISSN 1831-9424, Luxembourg., 2013.

Wiesmeier, M., Urbanski, L., Hobley, E., Lang, B., von Lützow, M., Marin-Spiotta, E., van Wesemael, B., Rabot, E., Ließ, M., Garcia-Franco, N., Wollschläger, U., Vogel, H. J. and Kögel-Knabner, I.: Soil organic carbon storage as a key function of soils - A review of drivers and indicators at various scales, Geoderma, 333, 149–162, doi:10.1016/j.geoderma.2018.07.026, 2019.

Wösten, J. H. M., Lilly, A., Nemes, A., Bas, C. Le and Le Bas, C.: Development and use of a database of hydraulic properties of European soils, Geoderma, 90(3–4), 169–185, 1999.

Wright, M. N. and Ziegler, A.: ranger: A Fast Implementation of Random Forests for High Dimensional Data in C++ and R, J. Stat. Softw., 77(1), doi:10.18637/jss.v077.i01, 2017.

Zhang, Y. and Schaap, M. G.: Weighted recalibration of the Rosetta pedotransfer model with improved estimates of hydraulic parameter distributions and summary statistics (Rosetta3), J. Hydrol., 547(January 2017), 39–53, doi:10.1016/j.jhydrol.2017.01.004, 2017.

Zhao, H., Zeng, Y., Lv, S. and Su, Z.: Analysis of soil hydraulic and thermal properties for land surface modeling over the Tibetan Plateau, Earth Syst. Sci. Data, 10(2), 1031–1061, doi:10.5194/essd-10-1031-2018, 2018.

Ziegler, A. and König, I. R.: Mining data with random forests: Current options for real-world applications, Wiley Interdiscip. Rev. Data Min. Knowl. Discov., 4(1), 55–63, doi:10.1002/widm.1114, 2014.

Preprints (www.preprints.org) | NOT PEER-REVIEWED | Posted: 28 February 2020 doi:10.20944/preprints202002.0425.v1

TABLES

Table 1. Number of samples by predictor variable combinations used to derive the new European PTFs (euptfv2). Rows in italic font indicate PTFs with the same predictor variables as were tested in euptfv1 (Tóth et al., 2015).

Name	Predictor variables[1]	Number of samples in TRAIN set[2]								
		THS	FC_2	FC	WP	KS	AWC_2	AWC	VG	MVG
PTF01	*PSD+DEPTH*	*3354*	*5109*	*2196*	*5264*	*3157*	*3528*	*1863*	*4669*	*739*
PTF02	*PSD+DEPTH+OC*	*2966*	*4131*	*1716*	*4802*	*2620*	*3208*	*1650*	*3708*	*407*
PTF03	PSD+DEPTH+BD	3305	5034	2176	5197	3146	3472	1849	4593	726
PTF04	PSD+DEPTH+CACO3	678	1670	1537	1816	639	1548	1531	1671	273
PTF05	PSD+DEPTH+PH_H2O	1203	2062	1278	2039	907	1849	1245	1897	230
PTF06	PSD+DEPTH+CEC	895	1649	1097	1703	567	1550	1092	1488	141
PTF07	*PSD+DEPTH+OC+BD*	*2959*	*4117*	*1711*	*4786*	*2609*	*3197*	*1645*	*3695*	*404*
PTF08	PSD+DEPTH+OC+CACO3	673	1586	1340	1599	613	1464	1336	1589	250
PTF09	PSD+DEPTH+OC+PH_H2O	1052	1808	1100	1678	862	1615	1074	1663	224
PTF10	PSD+DEPTH+OC+CEC	744	1437	1001	1459	525	1358	998	1293	138
PTF11	PSD+DEPTH+BD+CACO3	678	1666	1526	1806	639	1545	1522	1670	272
PTF12	PSD+DEPTH+BD+PH_H2O	1156	2008	1267	1979	898	1796	1236	1847	229
PTF13	PSD+DEPTH+BD+CEC	848	1596	1093	1648	558	1498	1088	1437	140
PTF14	PSD+DEPTH+CACO3+PH_H2O	678	1314	1235	1375	620	1195	1230	1264	223
PTF15	PSD+DEPTH+CACO3+CEC	373	770	793	831	405	726	791	758	136
PTF16	PSD+DEPTH+PH_H2O+CEC	894	1350	744	1349	567	1255	739	1188	141
PTF17	PSD+DEPTH+OC+BD+CACO3	673	1585	1338	1596	613	1464	1334	1588	249
PTF18	*PSD+DEPTH+OC+BD+PH_H2O*	*1047*	*1799*	*1098*	*1667*	*853*	*1607*	*1072*	*1655*	*223*
PTF19	PSD+DEPTH+OC+BD+CEC	739	1427	998	1447	516	1349	995	1284	137
PTF20	PSD+DEPTH+OC+CACO3+PH_H2O	673	1249	1062	1183	613	1130	1059	1201	219
PTF21	PSD+DEPTH+OC+CACO3+CEC	369	727	709	743	401	683	707	712	135
PTF22	PSD+DEPTH+OC+PH_H2O+CEC	744	1142	663	1121	525	1067	660	996	138
PTF23	PSD+DEPTH+BD+CACO3+PH_H2O	678	1310	1224	1365	620	1192	1221	1263	222
PTF24	PSD+DEPTH+BD+CACO3+CEC	373	768	790	827	405	725	788	757	135
PTF25	PSD+DEPTH+BD+PH_H2O+CEC	847	1298	741	1295	558	1204	736	1138	140
PTF26	PSD+DEPTH+CACO3+PH_H2O+CEC	373	727	734	772	405	684	732	717	136
PTF27	PSD+DEPTH+OC+BD+CACO3+PH_H2O	673	1248	1060	1180	613	1130	1057	1200	218
PTF28	PSD+DEPTH+OC+BD+CACO3+CEC	369	726	707	740	401	683	705	711	134
PTF29	PSD+DEPTH+OC+BD+PH_H2O+CEC	739	1133	661	1110	516	1059	658	988	137
PTF30	*PSD+DEPTH+OC+CACO3+PH_H2O+CEC*	*369*	*684*	*655*	*689*	*401*	*641*	*653*	*671*	*135*
PTF31	PSD+DEPTH+BD+CACO3+PH_H2O+CEC	373	725	731	768	405	683	729	716	135
PTF32	*PSD+DEPTH+OC+BD+CACO3+PH_H2O+CEC*	*369*	*683*	*653*	*686*	*401*	*641*	*651*	*670*	*134*
	Number of samples in TEST_BASIC set	1247	1762	801	2088	1117	1372	705	1591	176
	Number of samples in TEST_CHEM+ set	156	296	280	294	169	274	279	288	57

[1]PSD: particle size distribution (sand, 50–2000 µm; silt, 2–50 µm; clay, <2 µm (mass %)); DEPTH: mean soil depth (cm); OC: organic carbon content (mass %); BD: bulk density (g cm^{-3}); CACO3: calcium carbonate content (mass %); PH_H2O: pH in water (-); CEC: cation exchange capacity (cmol (+) kg^{-1}).

[2]THS: saturated water content (pF 0); FC_2: water content at -100 cm matric potential head (pF 2.0); FC: water content at -330 cm matric potential head (pF 2.5); AWC_2: plant available water content based on FC_2; AWC: plant available water content based on FC; WP: water content at wilting point (pF 4.2); KS: saturated hydraulic conductivity; VG: parameters of the van Genuchten model; MVG: parameters of the Mualem – van Genuchten model; TEST_BASIC: samples with measured PSD, DEPTH, OC and BD; TEST_CHEM+: samples with measured PSD, DEPTH, OC, BD, CACO3, PH_H2O and CEC.

Preprints (www.preprints.org) | NOT PEER-REVIEWED | Posted: 28 February 2020 doi:10.20944/preprints202002.0425.v1

Table 2. Performance of pedotransfer functions (PTFs) by input combination on training and test datasets to predict water content at saturation (THS). N: number of samples, RMSE: root mean square error **(**cm^3 cm^{-3}**)**, and R^2: determination coefficient, TEST_BASIC: samples with measured PSD, DEPTH, OC and BD; TEST_CHEM+: samples with measured PSD, DEPTH, OC, BD, CACO3, PH_H2O and CEC. Recommended PTFs are highlighted in bold.

Name of PTF in euptfv2	Predictor variables[1]	Training set			Test set			Sign. difference[2]			
		N	RMSE	R^2	N	RMSE	R^2	TEST_BASIC set	TEST_CHEM + set	Recommended PTF	Pair from euptfv1
PTF01	**PSD+DEPTH**	3354	0.067	0.366	1274	0.068	0.344	a	a	PTF01	-
PTF02	**PSD+DEPTH+OC**	2966	0.053	0.577	1274	0.056	0.552	b	abc	PTF02	PTF04
PTF03	**PSD+DEPTH+BD**	3305	0.029	0.880	1274	0.031	0.862	c	d	PTF03	-
PTF04	**PSD+DEPTH+CACO3**	678	0.046	0.187	156	0.057	0.053	-	bc	PTF04	-
PTF05	**PSD+DEPTH+PH_H2O**	1203	0.056	0.298	156	0.053	0.193	-	bc	PTF05	-
PTF06	PSD+DEPTH+CEC	895	0.055	0.401	156	0.057	0.048	-	ab	PTF01	-
PTF07	PSD+DEPTH+OC+BD	2959	0.027	0.888	1274	0.030	0.869	c	d	PTF03	PTF05
PTF08	PSD+DEPTH+OC+CACO3	673	0.044	0.209	156	0.055	0.118	-	bc	PTF02	-
PTF09	PSD+DEPTH+OC+PH_H2O	1052	0.046	0.457	156	0.050	0.272	-	c	PTF02	-
PTF10	PSD+DEPTH+OC+CEC	744	0.046	0.519	156	0.051	0.233	-	abc	PTF02	-
PTF11	PSD+DEPTH+BD+CACO3	678	0.023	0.791	156	0.022	0.863	-	d	PTF03	-
PTF12	PSD+DEPTH+BD+PH_H2O	1156	0.027	0.826	156	0.021	0.878	-	d	PTF03	-
PTF13	PSD+DEPTH+BD+CEC	848	0.027	0.848	156	0.021	0.873	-	d	PTF03	-
PTF14	PSD+DEPTH+CACO3+PH_H2O	678	0.045	0.231	156	0.050	0.265	-	bc	PTF05	-
PTF15	PSD+DEPTH+CACO3+CEC	373	0.045	0.257	156	0.054	0.164	-	abc	PTF04	-
PTF16	PSD+DEPTH+PH_H2O+CEC	894	0.052	0.459	156	0.055	0.132	-	bc	PTF05	-
PTF17	PSD+DEPTH+OC+BD+CACO3	673	0.019	0.856	156	0.021	0.872	-	d	PTF03	-
PTF18	PSD+DEPTH+OC+BD+PH_H2O	1047	0.024	0.848	156	0.021	0.871	-	d	PTF03	PTF06
PTF19	PSD+DEPTH+OC+BD+CEC	739	0.027	0.837	156	0.021	0.874	-	d	PTF03	-
PTF20	PSD+DEPTH+OC+CACO3+PH_H2O	673	0.043	0.251	156	0.050	0.285	-	c	PTF02	-
PTF21	PSD+DEPTH+OC+CACO3+CEC	369	0.043	0.309	156	0.051	0.242	-	bc	PTF02	-
PTF22	PSD+DEPTH+OC+PH_H2O+CEC	744	0.046	0.531	156	0.050	0.280	-	bc	PTF02	-
PTF23	PSD+DEPTH+BD+CACO3+PH_H2O	678	0.023	0.796	156	0.021	0.869	-	d	PTF03	-
PTF24	PSD+DEPTH+BD+CACO3+CEC	373	0.021	0.841	156	0.021	0.869	-	d	PTF03	-
PTF25	PSD+DEPTH+BD+PH_H2O+CEC	847	0.027	0.850	156	0.020	0.883	-	d	PTF03	-
PTF26	PSD+DEPTH+CACO3+PH_H2O+CEC	373	0.044	0.305	156	0.049	0.308	-	abc	PTF05	-
PTF27	PSD+DEPTH+OC+BD+CACO3+PH_H2O	673	0.019	0.858	156	0.022	0.865	-	d	PTF03	-
PTF28	PSD+DEPTH+OC+BD+CACO3+CEC	369	0.021	0.845	156	0.021	0.874	-	d	PTF03	-
PTF29	PSD+DEPTH+OC+BD+PH_H2O+CEC	739	0.026	0.843	156	0.020	0.880	-	d	PTF03	-
PTF30	PSD+DEPTH+OC+CACO3+PH_H2O+CEC	369	0.042	0.356	156	0.049	0.319	-	bc	PTF02	PTF04
PTF31	PSD+DEPTH+BD+CACO3+PH_H2O+CEC	373	0.021	0.843	156	0.021	0.871	-	d	PTF03	-
PTF32	PSD+DEPTH+OC+BD+CACO3+PH_H2O+CEC	369	0.021	0.844	156	0.021	0.876	-	d	PTF03	PTF06

[1]PSD: particle size distribution (sand, 50–2000 µm; silt, 2–50 µm; clay, <2 µm (mass %)); DEPTH: mean soil depth (cm); OC: organic carbon content (mass %); BD: bulk density (g cm^{-3}); CACO3: calcium carbonate content (mass %); PH_H2O: pH in water (-); CEC: cation exchange capacity (cmol (+) kg^{-1}).

[2]Different letters indicate significant differences at the 0.05 level between the accuracy of the methods based on the squared error;for example performance indicated with the letter c is significantly better than the one noted with letters b and a.

Preprints (www.preprints.org) | NOT PEER-REVIEWED | Posted: 28 February 2020 doi:10.20944/preprints202002.0425.v1

Table 3. Performance of pedotransfer functions (PTFs) by input combination on training and test datasets to predict water content at -100 cm matric potential head (FC_2). N: number of samples, RMSE: root mean square error **(**cm^3 cm^{-3}**)**, and R^2: determination coefficient, TEST_BASIC: samples with measured PSD, DEPTH, OC and BD; TEST_CHEM+: samples with measured PSD, DEPTH, OC, BD, CACO3, PH_H2O and CEC. Recommended PTFs are highlighted in bold. FC_2 was not analysed in euptfv1.

Name of PTF in euptfv2	Predictor variables[1]	Training set			Test set			Sign. difference[2]		Recommended PTF	Pair from euptf v1
		N	RMSE	R^2	N	RMSE	R^2	TEST_BASIC set	TEST_CHEM + set		
PTF01	**PSD+DEPTH**	5109	0.062	0.651	1762	0.060	0.669	a	a	PTF01	-
PTF02	**PSD+DEPTH+OC**	4131	0.057	0.711	1762	0.055	0.718	b	ab	PTF02	-
PTF03	**PSD+DEPTH+BD**	5034	0.053	0.750	1762	0.052	0.745	bc	bcdef	PTF03	-
PTF04	**PSD+DEPTH+CACO3**	1670	0.052	0.566	296	0.054	0.467	-	abcd	PTF01	-
PTF05	**PSD+DEPTH+PH_H2O**	2062	0.056	0.630	296	0.056	0.419	-	abc	PTF01	-
PTF06	**PSD+DEPTH+CEC**	1649	0.056	0.658	296	0.054	0.469	-	abcde	PTF01	-
PTF07	**PSD+DEPTH+OC+BD**	4117	0.051	0.769	1762	0.050	0.769	c	bcdefg	PTF03	-
PTF08	**PSD+DEPTH+OC+CACO3**	1586	0.050	0.589	296	0.049	0.565	-	bcdefgh	PTF02	-
PTF09	**PSD+DEPTH+OC+PH_H2O**	1808	0.050	0.679	296	0.048	0.581	-	bcdefg	PTF02	-
PTF10	PSD+DEPTH+OC+CEC	1437	0.051	0.688	296	0.049	0.554	-	cdefghij	PTF06	-
PTF11	**PSD+DEPTH+BD+CACO3**	1666	0.044	0.701	296	0.046	0.616	-	fghijklmn	PTF03	-
PTF12	**PSD+DEPTH+BD+PH_H2O**	2008	0.046	0.746	296	0.043	0.657	-	efghijkl	PTF03	-
PTF13	**PSD+DEPTH+BD+CEC**	1596	0.046	0.763	296	0.046	0.614	-	hijklmn	PTF13	-
PTF14	PSD+DEPTH+CACO3+PH_H2O	1314	0.051	0.600	296	0.051	0.528	-	bcdef	PTF05	-
PTF15	PSD+DEPTH+CACO3+CEC	770	0.052	0.605	296	0.051	0.520	-	cdefghij	PTF04	-
PTF16	PSD+DEPTH+PH_H2O+CEC	1350	0.053	0.699	296	0.049	0.556	-	cdefghi	PTF05	-
PTF17	PSD+DEPTH+OC+BD+CACO3	1585	0.043	0.689	296	0.045	0.634	-	ghijklmn	PTF07	-
PTF18	**PSD+DEPTH+OC+BD+PH_H2O**	1799	0.044	0.749	296	0.042	0.679	-	ghijklmn	PTF07	-
PTF19	PSD+DEPTH+OC+BD+CEC	1427	0.045	0.753	296	0.044	0.650	-	jklmn	PTF13	-
PTF20	PSD+DEPTH+OC+CACO3+PH_H2O	1249	0.049	0.613	296	0.053	0.483	-	bcdefgh	PTF02	-
PTF21	PSD+DEPTH+OC+CACO3+CEC	727	0.050	0.603	296	0.046	0.620	-	fghijklmn	PTF08	-
PTF22	PSD+DEPTH+OC+PH_H2O+CEC	1142	0.051	0.693	296	0.045	0.630	-	efghijklm	PTF09	-
PTF23	PSD+DEPTH+BD+CACO3+PH_H2O	1310	0.044	0.701	296	0.045	0.629	-	defghijkl	PTF03	-
PTF24	PSD+DEPTH+BD+CACO3+CEC	768	0.043	0.722	296	0.043	0.666	-	lmn	PTF11	-
PTF25	PSD+DEPTH+BD+PH_H2O+CEC	1298	0.046	0.773	296	0.043	0.668	-	jklmn	PTF12	-
PTF26	PSD+DEPTH+CACO3+PH_H2O+CEC	727	0.051	0.633	296	0.048	0.587	-	defghijk	PTF05	-
PTF27	PSD+DEPTH+OC+BD+CACO3+PH_H2O	1248	0.043	0.693	296	0.044	0.653	-	efghijklm	PTF07	-
PTF28	PSD+DEPTH+OC+BD+CACO3+CEC	726	0.044	0.702	296	0.041	0.687	-	klmn	PTF11	-
PTF29	PSD+DEPTH+OC+BD+PH_H2O+CEC	1133	0.046	0.757	296	0.042	0.681	-	ijklmn	PTF12	-
PTF30	PSD+DEPTH+OC+CACO3+PH_H2O+CEC	684	0.050	0.617	296	0.051	0.533	-	efghijklm	PTF09	-
PTF31	PSD+DEPTH+BD+CACO3+PH_H2O+CEC	725	0.043	0.731	296	0.041	0.698	-	mn	PTF11	-
PTF32	PSD+DEPTH+OC+BD+CACO3+PH_H2O+CEC	683	0.044	0.712	296	0.040	0.709	-	n	PTF18	-

[1]PSD: particle size distribution (sand, 50–2000 µm; silt, 2–50 µm; clay, <2 µm (mass %)); DEPTH: mean soil depth (cm); OC: organic carbon content (mass %); BD: bulk density (g cm^{-3}); CACO3: calcium carbonate content (mass %); PH_H2O: pH in water (-); CEC: cation exchange capacity (cmol (+) kg^{-1}).

[2]Different letters indicate significant differences at the 0.05 level between the accuracy of the methods based on the squared error;for example performance indicated with the letter c is significantly better than the one noted with letters b and a.

Preprints (www.preprints.org) | NOT PEER-REVIEWED | Posted: 28 February 2020 doi:10.20944/preprints202002.0425.v1

Table 4. Performance of pedotransfer functions (PTFs) by input combination on training and test datasets to predict water content at -330 cm matric potential head, field capacity (FC). N: number of samples, RMSE: root mean square error **(**cm^3 cm^{-3}**)**, and R^2: determination coefficient, TEST_BASIC: samples with measured PSD, DEPTH, OC and BD; TEST_CHEM+: samples with measured PSD, DEPTH, OC, BD, CACO3, PH_H2O and CEC. Recommended PTFs are highlighted in bold.

Name of PTF in euptfv2	Predictor variables[1]	Training set			Test set			Sign. difference[2]		Recommended PTF	Pair from euptfv1
		N	RMSE	R^2	N	RMSE	R^2	TEST_BASIC set	TEST_CHEM + set		
PTF01	**PSD+DEPTH**	2196	0.056	0.639	801	0.054	0.595	a	a	PTF01	-
PTF02	**PSD+DEPTH+OC**	1716	0.049	0.707	801	0.050	0.650	b	abc	PTF02	PTF09
PTF03	**PSD+DEPTH+BD**	2176	0.048	0.727	801	0.049	0.668	ab	abcd	PTF01	-
PTF04	**PSD+DEPTH+CACO3**	1537	0.047	0.650	280	0.055	0.591	-	abcde	PTF01	-
PTF05	PSD+DEPTH+PH_H2O	1278	0.048	0.653	280	0.055	0.586	-	ab	PTF01	-
PTF06	**PSD+DEPTH+CEC**	1097	0.046	0.711	280	0.052	0.630	-	bcdefghi	PTF06	-
PTF07	**PSD+DEPTH+OC+BD**	1711	0.046	0.736	801	0.048	0.677	b	bcdefg	PTF02	PTF09
PTF08	**PSD+DEPTH+OC+CACO3**	1340	0.043	0.678	280	0.053	0.616	-	abcdef	PTF02	-
PTF09	**PSD+DEPTH+OC+PH_H2O**	1100	0.044	0.687	280	0.052	0.631	-	abcde	PTF02	-
PTF10	PSD+DEPTH+OC+CEC	1001	0.044	0.720	280	0.052	0.628	-	bcdefghi	PTF02	-
PTF11	**PSD+DEPTH+BD+CACO3**	1526	0.044	0.696	280	0.051	0.649	-	bcdefgh	PTF03	-
PTF12	PSD+DEPTH+BD+PH_H2O	1267	0.045	0.698	280	0.050	0.658	-	bcdefgh	PTF03	-
PTF13	PSD+DEPTH+BD+CEC	1093	0.044	0.741	280	0.049	0.678	-	fghi	PTF06	-
PTF14	**PSD+DEPTH+CACO3+PH_H2O**	1235	0.048	0.667	280	0.053	0.623	-	bcdef	PTF04	-
PTF15	PSD+DEPTH+CACO3+CEC	793	0.047	0.720	280	0.052	0.639	-	efghi	PTF04	-
PTF16	PSD+DEPTH+PH_H2O+CEC	744	0.047	0.726	280	0.051	0.651	-	efghi	PTF06	-
PTF17	PSD+DEPTH+OC+BD+CACO3	1338	0.042	0.699	280	0.050	0.667	-	cdefghi	PTF02	-
PTF18	PSD+DEPTH+OC+BD+PH_H2O	1098	0.043	0.704	280	0.050	0.660	-	bcdefgh	PTF02	PTF09
PTF19	PSD+DEPTH+OC+BD+CEC	998	0.042	0.739	280	0.048	0.684	-	fghi	PTF07	-
PTF20	PSD+DEPTH+OC+CACO3+PH_H2O	1062	0.044	0.694	280	0.052	0.634	-	abcde	PTF02	-
PTF21	PSD+DEPTH+OC+CACO3+CEC	709	0.045	0.709	280	0.051	0.652	-	efghi	PTF04	-
PTF22	PSD+DEPTH+OC+PH_H2O+CEC	663	0.046	0.706	280	0.050	0.664	-	defghi	PTF09	-
PTF23	PSD+DEPTH+BD+CACO3+PH_H2O	1224	0.045	0.704	280	0.051	0.651	-	bcdefgh	PTF03	-
PTF24	PSD+DEPTH+BD+CACO3+CEC	790	0.044	0.744	280	0.048	0.688	-	hi	PTF11	-
PTF25	PSD+DEPTH+BD+PH_H2O+CEC	741	0.045	0.748	280	0.048	0.682	-	hi	PTF11	-
PTF26	PSD+DEPTH+CACO3+PH_H2O+CEC	734	0.046	0.742	280	0.050	0.658	-	fghi	PTF14	-
PTF27	PSD+DEPTH+OC+BD+CACO3+PH_H2O	1060	0.042	0.712	280	0.049	0.676	-	bcdefghi	PTF02	-
PTF28	PSD+DEPTH+OC+BD+CACO3+CEC	707	0.043	0.731	280	0.048	0.693	-	ghi	PTF07	-
PTF29	PSD+DEPTH+OC+BD+PH_H2O+CEC	661	0.044	0.725	280	0.046	0.709	-	fghi	PTF07	-
PTF30	PSD+DEPTH+OC+CACO3+PH_H2O+CEC	655	0.044	0.731	280	0.049	0.672	-	fghi	PTF08	PTF09
PTF31	PSD+DEPTH+BD+CACO3+PH_H2O+CEC	731	0.043	0.763	280	0.047	0.700	-	i	PTF06	-
PTF32	PSD+DEPTH+OC+BD+CACO3+PH_H2O+CEC	653	0.043	0.743	280	0.047	0.696	-	fghi	PTF07	PTF09

[1]PSD: particle size distribution (sand, 50–2000 µm; silt, 2–50 µm; clay, <2 µm (mass %)); DEPTH: mean soil depth (cm); OC: organic carbon content (mass %); BD: bulk density (g cm^{-3}); CACO3: calcium carbonate content (mass %); PH_H2O: pH in water (-); CEC: cation exchange capacity (cmol (+) kg^{-1}).

[2]Different letters indicate significant differences at the 0.05 level between the accuracy of the methods based on the squared error;for example performance indicated with the letter c is significantly better than the one noted with letters b and a.

Preprints (www.preprints.org) | NOT PEER-REVIEWED | Posted: 28 February 2020 doi:10.20944/preprints202002.0425.v1

Table 5. Performance of pedotransfer functions (PTFs) by input combination on training and test datasets to predict water content at wilting point (WP). N: number of samples, RMSE: root mean square error **(**cm^3 cm^{-3}**)**, and R^2: determination coefficient, TEST_BASIC: samples with measured PSD, DEPTH, OC and BD; TEST_CHEM+: samples with measured PSD, DEPTH, OC, BD, CACO3, PH_H2O and CEC. Recommended PTFs are highlighted in bold.

Name of PTF in euptfv2	Predictor variables[1]	Training set			Test set			Sign. difference[2]		Recommended PTF	Pair from euptfv1
		N	RMSE	R^2	N	RMSE	R^2	TEST_BASIC set	TEST_CHEM + set		
PTF01	**PSD+DEPTH**	5264	0.048	0.736	2088	0.048	0.728	a	a	PTF01	-
PTF02	**PSD+DEPTH+OC**	4802	0.047	0.755	2088	0.046	0.745	bc	abc	PTF02	PTF12
PTF03	PSD+DEPTH+BD	5197	0.046	0.757	2088	0.046	0.754	ab	ab	PTF01	-
PTF04	PSD+DEPTH+CACO3	1816	0.042	0.693	294	0.042	0.643	-	a	PTF01	-
PTF05	PSD+DEPTH+PH_H2O	2039	0.046	0.673	294	0.044	0.621	-	abc	PTF01	-
PTF06	PSD+DEPTH+CEC	1703	0.043	0.725	294	0.041	0.662	-	a	PTF01	-
PTF07	**PSD+DEPTH+OC+BD**	4786	0.045	0.769	2088	0.044	0.769	c	abc	PTF02	PTF12
PTF08	**PSD+DEPTH+OC+CACO3**	1599	0.041	0.695	294	0.041	0.671	-	abcd	PTF02	-
PTF09	**PSD+DEPTH+OC+PH_H2O**	1678	0.045	0.682	294	0.041	0.661	-	abcd	PTF02	-
PTF10	PSD+DEPTH+OC+CEC	1459	0.043	0.704	294	0.040	0.674	-	abcd	PTF02	-
PTF11	PSD+DEPTH+BD+CACO3	1806	0.041	0.706	294	0.040	0.682	-	abcd	PTF01	-
PTF12	PSD+DEPTH+BD+PH_H2O	1979	0.045	0.691	294	0.041	0.671	-	abcd	PTF01	-
PTF13	PSD+DEPTH+BD+CEC	1648	0.042	0.729	294	0.040	0.683	-	abcd	PTF01	-
PTF14	PSD+DEPTH+CACO3+PH_H2O	1375	0.043	0.689	294	0.042	0.649	-	abcd	PTF01	-
PTF15	PSD+DEPTH+CACO3+CEC	831	0.044	0.657	294	0.039	0.694	-	abcd	PTF01	-
PTF16	PSD+DEPTH+PH_H2O+CEC	1349	0.043	0.727	294	0.040	0.681	-	abc	PTF01	-
PTF17	**PSD+DEPTH+OC+BD+CACO3**	1596	0.041	0.705	294	0.039	0.702	-	abcd	PTF07	-
PTF18	PSD+DEPTH+OC+BD+PH_H2O	1667	0.045	0.687	294	0.040	0.674	-	abcd	PTF07	PTF12
PTF19	PSD+DEPTH+OC+BD+CEC	1447	0.042	0.714	294	0.039	0.691	-	abcd	PTF07	-
PTF20	PSD+DEPTH+OC+CACO3+PH_H2O	1183	0.042	0.691	294	0.040	0.686	-	abcd	PTF02	-
PTF21	PSD+DEPTH+OC+CACO3+CEC	743	0.044	0.638	294	0.037	0.722	-	d	PTF08	-
PTF22	PSD+DEPTH+OC+PH_H2O+CEC	1121	0.044	0.697	294	0.039	0.701	-	abcd	PTF07	-
PTF23	PSD+DEPTH+BD+CACO3+PH_H2O	1365	0.042	0.701	294	0.040	0.678	-	abcd	PTF01	-
PTF24	PSD+DEPTH+BD+CACO3+CEC	827	0.043	0.673	294	0.038	0.708	-	abcd	PTF01	-
PTF25	PSD+DEPTH+BD+PH_H2O+CEC	1295	0.043	0.726	294	0.039	0.698	-	abcd	PTF01	-
PTF26	PSD+DEPTH+CACO3+PH_H2O+CEC	772	0.043	0.680	294	0.039	0.702	-	cd	PTF05	-
PTF27	PSD+DEPTH+OC+BD+CACO3+PH_H2O	1180	0.042	0.698	294	0.039	0.703	-	abcd	PTF07	-
PTF28	PSD+DEPTH+OC+BD+CACO3+CEC	740	0.043	0.648	294	0.037	0.732	-	bcd	PTF17	-
PTF29	PSD+DEPTH+OC+BD+PH_H2O+CEC	1110	0.043	0.699	294	0.038	0.712	-	abcd	PTF07	-
PTF30	PSD+DEPTH+OC+CACO3+PH_H2O+CEC	689	0.044	0.645	294	0.038	0.719	-	abcd	PTF02	PTF12
PTF31	PSD+DEPTH+BD+CACO3+PH_H2O+CEC	768	0.043	0.678	294	0.037	0.720	-	cd	PTF05	-
PTF32	PSD+DEPTH+OC+BD+CACO3+PH_H2O+CEC	686	0.043	0.656	294	0.037	0.723	-	d	PTF09	PTF12

[1]PSD: particle size distribution (sand, 50–2000 µm; silt, 2–50 µm; clay, <2 µm (mass %)); DEPTH: mean soil depth (cm); OC: organic carbon content (mass %); BD: bulk density (g cm^{-3}); CACO3: calcium carbonate content (mass %); PH_H2O: pH in water (-); CEC: cation exchange capacity (cmol (+) kg^{-1}).

[2]Different letters indicate significant differences at the 0.05 level between the accuracy of the methods based on the squared error;for example performance indicated with the letter c is significantly better than the one noted with letters b and a.

Preprints (www.preprints.org) | NOT PEER-REVIEWED | Posted: 28 February 2020 doi:10.20944/preprints202002.0425.v1

Table 6. Performance of pedotransfer functions (PTFs) by input combination on training and test datasets to predict saturated hydraulic conductivity (KS). N: number of samples, RMSE: root mean square error (log_{10} (cm day^{-1})), and R^2: determination coefficient, TEST_BASIC: samples with measured PSD, DEPTH, OC and BD; TEST_CHEM+: samples with measured PSD, DEPTH, OC, BD, CACO3, PH_H2O and CEC. Recommended PTFs are highlighted in bold.

Name of PTF in euptfv2	Predictor variables[1]	Training set			Test set			Sign. difference[2]		Recommended PTF	Pair from euptfv1
		N	RMSE	R^2	N	RMSE	R^2	TEST_BASIC set	TEST_CHEM + set		
PTF01	**PSD+DEPTH**	3157	1.200	0.434	1117	1.181	0.307	a	ab	PTF01	-
PTF02	**PSD+DEPTH+OC**	2620	0.957	0.566	1117	0.953	0.548	b	bc	PTF02	PTF16
PTF03	PSD+DEPTH+BD	3146	1.160	0.467	1117	1.170	0.320	a	a	PTF01	-
PTF04	PSD+DEPTH+CACO3	639	0.861	0.241	169	0.959	0.123	-	abc	PTF01	-
PTF05	**PSD+DEPTH+PH_H2O**	907	0.875	0.213	169	0.944	0.151	-	bc	PTF01	-
PTF06	PSD+DEPTH+CEC	567	0.984	0.215	169	0.940	0.157	-	bc	PTF01	-
PTF07	PSD+DEPTH+OC+BD	2609	0.931	0.590	1117	0.939	0.562	b	bc	PTF02	PTF16
PTF08	PSD+DEPTH+OC+CACO3	613	0.872	0.244	169	0.943	0.153	-	bc	PTF02	-
PTF09	PSD+DEPTH+OC+PH_H2O	862	0.847	0.257	169	0.938	0.162	-	bc	PTF02	-
PTF10	PSD+DEPTH+OC+CEC	525	0.977	0.223	169	0.938	0.162	-	bc	PTF02	-
PTF11	PSD+DEPTH+BD+CACO3	639	0.851	0.259	169	0.952	0.136	-	bc	PTF01	-
PTF12	PSD+DEPTH+BD+PH_H2O	898	0.853	0.256	169	0.947	0.145	-	bc	PTF05	-
PTF13	PSD+DEPTH+BD+CEC	558	0.980	0.230	169	0.941	0.157	-	bc	PTF01	-
PTF14	PSD+DEPTH+CACO3+PH_H2O	620	0.855	0.267	169	0.923	0.189	-	bc	PTF05	-
PTF15	PSD+DEPTH+CACO3+CEC	405	0.937	0.263	169	0.941	0.156	-	abc	PTF01	-
PTF16	PSD+DEPTH+PH_H2O+CEC	567	0.942	0.282	169	0.940	0.158	-	bc	PTF01	-
PTF17	PSD+DEPTH+OC+BD+CACO3	613	0.856	0.272	169	0.933	0.171	-	bc	PTF02	-
PTF18	PSD+DEPTH+OC+BD+PH_H2O	853	0.831	0.289	169	0.932	0.172	-	bc	PTF02	PTF16
PTF19	PSD+DEPTH+OC+BD+CEC	516	0.979	0.228	169	0.928	0.179	-	c	PTF02	-
PTF20	PSD+DEPTH+OC+CACO3+PH_H2O	613	0.860	0.264	169	0.929	0.177	-	bc	PTF02	-
PTF21	PSD+DEPTH+OC+CACO3+CEC	401	0.935	0.271	169	0.925	0.184	-	bc	PTF02	-
PTF22	PSD+DEPTH+OC+PH_H2O+CEC	525	0.931	0.295	169	0.933	0.170	-	c	PTF02	-
PTF23	PSD+DEPTH+BD+CACO3+PH_H2O	620	0.844	0.286	169	0.889	0.247	-	c	PTF05	-
PTF24	PSD+DEPTH+BD+CACO3+CEC	405	0.922	0.286	169	0.958	0.125	-	abc	PTF01	-
PTF25	PSD+DEPTH+BD+PH_H2O+CEC	558	0.944	0.286	169	0.950	0.140	-	bc	PTF05	-
PTF26	PSD+DEPTH+CACO3+PH_H2O+CEC	405	0.922	0.286	169	0.922	0.190	-	bc	PTF05	-
PTF27	PSD+DEPTH+OC+BD+CACO3+PH_H2O	613	0.844	0.293	169	0.893	0.241	-	c	PTF02	-
PTF28	PSD+DEPTH+OC+BD+CACO3+CEC	401	0.926	0.285	169	0.925	0.185	-	abc	PTF02	-
PTF29	PSD+DEPTH+OC+BD+PH_H2O+CEC	516	0.932	0.301	169	0.921	0.193	-	bc	PTF02	-
PTF30	PSD+DEPTH+OC+CACO3+PH_H2O+CEC	401	0.931	0.278	169	0.887	0.250	-	bc	PTF02	PTF17
PTF31	PSD+DEPTH+BD+CACO3+PH_H2O+CEC	405	0.914	0.298	169	0.912	0.207	-	bc	PTF05	-
PTF32	PSD+DEPTH+OC+BD+CACO3+PH_H2O+CEC	401	0.921	0.292	169	0.916	0.201	-	bc	PTF02	PTF17

[1]PSD: particle size distribution (sand, 50–2000 µm; silt, 2–50 µm; clay, <2 µm (mass %)); DEPTH: mean soil depth (cm); OC: organic carbon content (mass %); BD: bulk density (g cm^{-3}); CACO3: calcium carbonate content (mass %); PH_H2O: pH in water (-); CEC: cation exchange capacity (cmol (+) kg^{-1}).

[2]Different letters indicate significant differences at the 0.05 level between the accuracy of the methods based on the squared error;for example performance indicated with the letter c is significantly better than the one noted with letters b and a.

Preprints (www.preprints.org) | NOT PEER-REVIEWED | Posted: 28 February 2020 doi:10.20944/preprints202002.0425.v1

Table 7. Performance of pedotransfer functions (PTFs) by input combination on training and test datasets to predict parameters of the van Genuchten model to describe soil moisture retention curve (VG). N: number of samples, RMSE: root mean square error ($\log_{10}$ (cm day^{-1})), and R^2: determination coefficient, TEST_BASIC: samples with measured PSD, DEPTH, OC and BD; TEST_CHEM+: samples with measured PSD, DEPTH, OC, BD, CACO3, PH_H2O and CEC. Recommended PTFs are highlighted in bold.

Name of PTF in euptfv2	Predictor variables[1]	Training set			Test set			Sign. difference[2]		Recommended PTF	Pair from euptfv1
		N	RMSE	R^2	N	RMSE	R^2	TEST_BASIC set	TEST_CHEM + set		
PTF01	**PSD+DEPTH**	4669	0.055	0.846	1591	0.068	0.776	a	a	PTF01	-
PTF02	**PSD+DEPTH+OC**	3708	0.047	0.887	1591	0.060	0.826	b	c	PTF02	PTF19
PTF03	**PSD+DEPTH+BD**	4593	0.041	0.913	1591	0.056	0.846	c	hi	PTF03	-
PTF04	**PSD+DEPTH+CACO3**	1671	0.039	0.911	288	0.052	0.852	-	d	PTF04	-
PTF05	**PSD+DEPTH+PH_H2O**	1897	0.045	0.894	288	0.055	0.834	-	b	PTF05	-
PTF06	**PSD+DEPTH+CEC**	1488	0.044	0.886	288	0.054	0.839	-	d	PTF06	-
PTF07	**PSD+DEPTH+OC+BD**	3695	0.037	0.933	1591	0.054	0.859	d	fg	PTF07	PTF21
PTF08	**PSD+DEPTH+OC+CACO3**	1589	0.036	0.924	288	0.048	0.871	-	f	PTF08	-
PTF09	**PSD+DEPTH+OC+PH_H2O**	1663	0.039	0.922	288	0.050	0.865	-	gh	PTF09	-
PTF10	**PSD+DEPTH+OC+CEC**	1293	0.036	0.920	288	0.051	0.858	-	fg	PTF10	-
PTF11	**PSD+DEPTH+BD+CACO3**	1670	0.034	0.934	288	0.043	0.900	-	mn	PTF11	-
PTF12	**PSD+DEPTH+BD+PH_H2O**	1847	0.038	0.926	288	0.044	0.892	-	l	PTF12	-
PTF13	**PSD+DEPTH+BD+CEC**	1437	0.039	0.908	288	0.044	0.892	-	lm	PTF13	-
PTF14	**PSD+DEPTH+CACO3+PH_H2O**	1264	0.037	0.928	288	0.052	0.854	-	e	PTF14	-
PTF15	**PSD+DEPTH+CACO3+CEC**	758	0.040	0.907	288	0.049	0.870	-	ij	PTF15	-
PTF16	**PSD+DEPTH+PH_H2O+CEC**	1188	0.042	0.905	288	0.051	0.858	-	f	PTF16	-
PTF17	PSD+DEPTH+OC+BD+CACO3	1588	0.031	0.944	288	0.042	0.904	-	n	PTF11	-
PTF18	PSD+DEPTH+OC+BD+PH_H2O	1655	0.033	0.943	288	0.043	0.900	-	l	PTF12	PTF22
PTF19	PSD+DEPTH+OC+BD+CEC	1284	0.033	0.934	288	0.044	0.892	-	lm	PTF13	-
PTF20	PSD+DEPTH+OC+CACO3+PH_H2O	1201	0.033	0.943	288	0.048	0.874	-	f	PTF09	-
PTF21	**PSD+DEPTH+OC+CACO3+CEC**	712	0.035	0.932	288	0.047	0.881	-	l	PTF21	-
PTF22	**PSD+DEPTH+OC+PH_H2O+CEC**	996	0.033	0.939	288	0.049	0.869	-	i	PTF22	-
PTF23	PSD+DEPTH+BD+CACO3+PH_H2O	1263	0.032	0.948	288	0.044	0.895	-	lm	PTF11	-
PTF24	**PSD+DEPTH+BD+CACO3+CEC**	757	0.033	0.939	288	0.041	0.906	-	o	PTF24	-
PTF25	**PSD+DEPTH+BD+PH_H2O+CEC**	1138	0.038	0.922	288	0.042	0.902	-	n	PTF25	-
PTF26	PSD+DEPTH+CACO3+PH_H2O+CEC	717	0.037	0.924	288	0.047	0.878	-	jk	PTF15	-
PTF27	PSD+DEPTH+OC+BD+CACO3+PH_H2O	1200	0.030	0.953	288	0.043	0.897	-	lm	PTF11	-
PTF28	PSD+DEPTH+OC+BD+CACO3+CEC	711	0.032	0.941	288	0.041	0.906	-	o	PTF24	-
PTF29	**PSD+DEPTH+OC+BD+PH_H2O+CEC**	988	0.032	0.945	288	0.041	0.906	-	o	PTF29	-
PTF30	PSD+DEPTH+OC+CACO3+PH_H2O+CEC	671	0.031	0.946	288	0.047	0.880	-	k	PTF21	PTF20
PTF31	PSD+DEPTH+BD+CACO3+PH_H2O+CEC	716	0.031	0.948	288	0.042	0.904	-	o	PTF24	-
PTF32	PSD+DEPTH+OC+BD+CACO3+PH_H2O+CEC	670	0.031	0.948	288	0.042	0.903	-	o	PTF29	PTF22

[1]PSD: particle size distribution (sand, 50–2000 µm; silt, 2–50 µm; clay, <2 µm (mass %)); DEPTH: mean soil depth (cm); OC: organic carbon content (mass %); BD: bulk density (g cm^{-3}); CACO3: calcium carbonate content (mass %); PH_H2O: pH in water (-); CEC: cation exchange capacity (cmol (+) kg^{-1}).

[2]Different letters indicate significant differences at the 0.05 level between the accuracy of the methods based on the squared error;for example performance indicated with the letter c is significantly better than the one noted with letters b and a.

Preprints (www.preprints.org) | NOT PEER-REVIEWED | Posted: 28 February 2020 doi:10.20944/preprints202002.0425.v1

Table 8. Performance of pedotransfer functions (PTFs) by input combination on training and test datasets to predict parameters of the Mualem-van Genuchten model to describe soil moisture retention and hydraulic conductivity curve (MVG). N: number of samples, RMSE: root mean square error (log_{10} (cm day^{-1})), and R^2: determination coefficient, TEST_BASIC: samples with measured PSD, DEPTH, OC and BD; TEST_CHEM+: samples with measured PSD, DEPTH, OC, BD, CACO3, PH_H2O and CEC. Recommended PTFs are highlighted in bold.

Name of PTF in euptfv2	Predictor variables[1]	Training set			Test set			Sign. difference[2]		Recommended PTF	Pair from euptfv1
		N	RMSE	R^2	N	RMSE	R^2	TEST_BASIC set	TEST_CHEM + set		
PTF01	**PSD+DEPTH**	739	0.604	0.804	176	0.708	0.796	a	b	PTF01	-
PTF02	**PSD+DEPTH+OC**	407	0.619	0.829	176	0.676	0.814	b	jkl	PTF02	PTF19
PTF03	PSD+DEPTH+BD	726	0.568	0.824	176	0.688	0.808	a	ab	PTF01	-
PTF04	**PSD+DEPTH+CACO3**	273	0.587	0.878	57	0.644	0.863	-	ijk	PTF04	-
PTF05	**PSD+DEPTH+PH_H2O**	230	0.578	0.889	57	0.663	0.855	-	def	PTF05	-
PTF06	**PSD+DEPTH+CEC**	141	0.672	0.858	57	0.662	0.856	-	fghij	PTF06	-
PTF07	PSD+DEPTH+OC+BD	404	0.529	0.873	176	0.659	0.824	b	a	PTF02	PTF19
PTF08	PSD+DEPTH+OC+CACO3	250	0.587	0.880	57	0.699	0.839	-	b	PTF02	-
PTF09	PSD+DEPTH+OC+PH_H2O	224	0.597	0.882	57	0.686	0.845	-	fghi	PTF02	-
PTF10	PSD+DEPTH+OC+CEC	138	0.699	0.846	57	0.702	0.837	-	cde	PTF02	-
PTF11	PSD+DEPTH+BD+CACO3	272	0.542	0.895	57	0.637	0.866	-	defg	PTF04	-
PTF12	**PSD+DEPTH+BD+PH_H2O**	229	0.520	0.909	57	0.620	0.873	-	jklm	PTF12	-
PTF13	**PSD+DEPTH+BD+CEC**	140	0.644	0.866	57	0.637	0.866	-	lm	PTF13	-
PTF14	PSD+DEPTH+CACO3+PH_H2O	223	0.539	0.904	57	0.691	0.842	-	c	PTF04	-
PTF15	PSD+DEPTH+CACO3+CEC	136	0.735	0.830	57	0.684	0.846	-	c	PTF04	-
PTF16	PSD+DEPTH+PH_H2O+CEC	141	0.666	0.860	57	0.666	0.854	-	hijk	PTF06	-
PTF17	PSD+DEPTH+OC+BD+CACO3	249	0.526	0.902	57	0.662	0.855	-	ab	PTF02	-
PTF18	PSD+DEPTH+OC+BD+PH_H2O	223	0.553	0.897	57	0.642	0.864	-	klm	PTF02	PTF19
PTF19	PSD+DEPTH+OC+BD+CEC	137	0.619	0.876	57	0.676	0.849	-	b	PTF02	-
PTF20	**PSD+DEPTH+OC+CACO3+PH_H2O**	219	0.573	0.891	57	0.661	0.856	-	n	PTF20	-
PTF21	**PSD+DEPTH+OC+CACO3+CEC**	135	0.730	0.831	57	0.653	0.86	-	m	PTF21	-
PTF22	PSD+DEPTH+OC+PH_H2O+CEC	138	0.699	0.846	57	0.664	0.855	-	lm	PTF02	-
PTF23	**PSD+DEPTH+BD+CACO3+PH_H2O**	222	0.515	0.911	57	0.639	0.865	-	lm	PTF23	-
PTF24	PSD+DEPTH+BD+CACO3+CEC	135	0.678	0.852	57	0.656	0.858	-	c	PTF04	-
PTF25	PSD+DEPTH+BD+PH_H2O+CEC	140	0.595	0.885	57	0.646	0.862	-	ghijk	PTF12	-
PTF26	PSD+DEPTH+CACO3+PH_H2O+CEC	136	0.712	0.841	57	0.669	0.852	-	cd	PTF04	-
PTF27	**PSD+DEPTH+OC+BD+CACO3+PH_H2O**	218	0.524	0.907	57	0.606	0.879	-	o	PTF27	-
PTF28	**PSD+DEPTH+OC+BD+CACO3+CEC**	134	0.656	0.860	57	0.639	0.865	-	n	PTF28	-
PTF29	**PSD+DEPTH+OC+BD+PH_H2O+CEC**	137	0.646	0.865	57	0.638	0.866	-	n	PTF29	-
PTF30	PSD+DEPTH+OC+CACO3+PH_H2O+CEC	135	0.726	0.833	57	0.680	0.847	-	fghi	PTF20	PTF19
PTF31	PSD+DEPTH+BD+CACO3+PH_H2O+CEC	135	0.679	0.851	57	0.668	0.853	-	c	PTF12	-
PTF32	PSD+DEPTH+OC+BD+CACO3+PH_H2O+CEC	134	0.645	0.864	57	0.678	0.848	-	efgh	PTF27	PTF19

[1]PSD: particle size distribution (sand, 50–2000 µm; silt, 2–50 µm; clay, <2 µm (mass %)); DEPTH: mean soil depth (cm); OC: organic carbon content (mass %); BD: bulk density (g cm^{-3}); CACO3: calcium carbonate content (mass %); PH_H2O: pH in water (-); CEC: cation exchange capacity (cmol (+) kg^{-1}).

[2]Different letters indicate significant differences at the 0.05 level between the accuracy of the methods based on the squared error;for example performance indicated with the letter c is significantly better than the one noted with letters b and a.

Preprints (www.preprints.org) | NOT PEER-REVIEWED | Posted: 28 February 2020 doi:10.20944/preprints202002.0425.v1

Table 9. The results of comparing the performance of parametric and point pedotransfer functions (PTFs) on the test sets of EU-HYDI to predict saturated water content (THS), water content at -100 cm matric potential head (FC_2), water content at -330 cm matric potential head (FC), water content at wilting point (WP). Rows in italic indicate cases where there was no significant difference between the two PTFs.

Predicted soil hydraulic property	Available predictor variables[1]	Performance of parameter estimation (MRC with VG)[2]		Performance of point estimation		Number of samples in test dataset
		Recommended PTF number	RMSE	Recommended PTF number	RMSE	
THS (cm^3 cm^{-3})	*PSD+DEPTH_M+OC*	*PTF02[a]*	*0.065*	*PTF02[a]*	*0.061*	*216*
	PSD+DEPTH_M+OC+BD	PTF07[a]	0.041	PTF03[b]	0.032	216
	PSD+DEPTH_M+OC+BD+PH_H2O	PTF12[a]	0.028	PTF03[b]	0.022	63
	PSD+DEPTH_M+OC+CACO3+PH_H2O+CEC	*PTF21[a]*	*0.051*	*PTF02[a]*	*0.060*	*63*
	PSD+DEPTH_M+OC+BD+CACO3+PH_H2O+CEC	*PTF29[a]*	*0.028*	*PTF03[a]*	*0.022*	*63*
FC_2 (cm^3 cm^{-3})	PSD+DEPTH_M+OC	PTF02[a]	0.057	PTF02[b]	0.054	424
	PSD+DEPTH_M+OC+BD	*PTF07[a]*	*0.051*	*PTF03[a]*	*0.051*	*424*
	PSD+DEPTH_M+OC+BD+PH_H2O	*PTF12[a]*	*0.043*	*PTF07[a]*	*0.049*	*68*
	PSD+DEPTH_M+OC+CACO3+PH_H2O+CEC	*PTF21[a]*	*0.043*	*PTF09[a]*	*0.047*	*68*
	PSD+DEPTH_M+OC+BD+CACO3+PH_H2O+CEC	*PTF29[a]*	*0.036*	*PTF18[a]*	*0.043*	*68*
FC (cm^3 cm^{-3})	*PSD+DEPTH_M+OC*	*PTF02[a]*	*0.057*	*PTF02[a]*	*0.048*	*319*
	PSD+DEPTH_M+OC+BD	*PTF07[a]*	*0.056*	*PTF02[a]*	*0.048*	*319*
	PSD+DEPTH_M+OC+BD+PH_H2O	*PTF12[a]*	*0.047*	*PTF02[a]*	*0.047*	*129*
	PSD+DEPTH_M+OC+CACO3+PH_H2O+CEC	*PTF21[a]*	*0.046*	*PTF08[a]*	*0.045*	*129*
	PSD+DEPTH_M+OC+BD+CACO3+PH_H2O+CEC	*PTF29[a]*	*0.041*	*PTF07[a]*	*0.046*	*129*
WP (cm^3 cm^{-3})	PSD+DEPTH_M+OC	PTF02[a]	0.064	PTF02[b]	0.047	429
	PSD+DEPTH_M+OC+BD	PTF07[a]	0.061	PTF02[b]	0.047	429
	PSD+DEPTH_M+OC+BD+PH_H2O	*PTF12a*	*0.053*	*PTF07[a]*	*0.045*	*91*
	PSD+DEPTH_M+OC+CACO3+PH_H2O+CEC	*PTF21[a]*	*0.051*	*PTF07[a]*	*0.045*	*91*
	PSD+DEPTH_M+OC+BD+CACO3+PH_H2O+CEC	*PTF29[a]*	*0.054*	*PTF09[a]*	*0.039*	*91*

[1]PSD: particle size distribution (sand, 50–2000 µm; silt, 2–50 µm; clay, <2 µm (mass %)); DEPTH: mean soil depth (cm); OC: organic carbon content (mass %); BD: bulk density (g cm^{-3}); CACO3: calcium carbonate content (mass %); PH_H2O: pH in water (-); CEC: cation exchange capacity (cmol (+) kg^{-1}).

[2]MRC: moisture retention curve; VG: parameters of the van Genuchten model. Different letters in a row indicate significant differences at the 0.05 level between the accuracy of the methods based on the squared error; for example performance indicated with the letter b is significantly better than the one noted with letter a. RMSE: root mean squared error.

Preprints (www.preprints.org) | NOT PEER-REVIEWED | Posted: 28 February 2020 doi:10.20944/preprints202002.0425.v1

Table 10. The results of comparing the performance of euptfv1 and euptfv2 on the test sets of EU-HYDI to predict soil hydraulic properties. Rows in italic indicate cases where there was no significant difference between the two PTFs.

Predicted soil hydraulic property[1]	Performance[2]					
	euptfv1		euptfv2		Name of test set	Number of samples in test datasets
	Name of PTF	RMSE	Name of PTF	RMSE		
THS	PTF04[a]	0.063	PTF02[b]	0.056	TEST_BASIC	1274
(cm^3 cm^{-3})	PTF05[a]	0.034	PTF03[b]	0.031	TEST_BASIC	1274
	PTF06[a]	*0.020*	*PTF03[a]*	*0.024*	*TEST_CHEM+*	*156*
FC	PTF09[a]	0.054	PTF02[b]	0.050	TEST_BASIC	801
(cm^3 cm^{-3})	PTF09[a]	0.054	PTF07[b]	0.048	TEST_BASIC	801
	PTF09[a]	0.058	PTF08[b]	0.053	TEST_CHEM+	280
WP	PTF12[a]	0.048	PTF02[b]	0.046	TEST_BASIC	2088
(cm^3 cm^{-3})	PTF12[a]	0.048	PTF07[b]	0.044	TEST_BASIC	2088
	PTF12[a]	*0.043*	*PTF09[a]*	*0.041*	*TEST_CHEM+*	*294*
KS	PTF16[a]	1.06	PTF02[b]	0.95	TEST_BASIC	1117
(log_{10} cm day^{-1})	*PTF17[a]*	*1.00*	*PTF02[a]*	*0.91*	*TEST_CHEM+*	*169*
VG	PTF19[a]	0.068	PTF02[b]	0.060	TEST_BASIC	1591
(cm^3 cm^{-3})	PTF21[a]	0.064	PTF07[b]	0.054	TEST_BASIC	1591
	PTF22[a]	0.046	PTF12[b]	0.044	TEST_CHEM+	288
	PTF20[a]	0.054	PTF21[b]	0.047	TEST_CHEM+	288
	PTF22[a]	0.046	PTF29[b]	0.041	TEST_CHEM+	288
MVG	PTF19[a]	0.77	PTF02[b]	0.68	TEST_BASIC	176
(log_{10} cm day^{-1})	*PTF19[a]*	*0.66*	*PTF20[a]*	*0.66*	*TEST_CHEM+*	*57*
	PTF19[a]	*0.66*	*PTF27[a]*	*0.61*	*TEST_CHEM+*	*57*

[1]THS: saturated water content (pF 0); FC_2: water content at -100 cm matric potential head (pF 2.0); FC: water content at -330 cm matric potential head (pF 2.5); WP: water content at wilting point (pF 4.2); KS: saturated hydraulic conductivity; VG: parameters of the van Genuchten model; MVG: parameters of the Mualem – van Genuchten model.

[2]Different letters in a row indicate significant differences at the 0.05 level between the accuracy of the methods based on the squared error;for example performance indicated with the letter b is significantly better than the one noted with letter a. RMSE: root mean squared error; TEST_BASIC: samples with measured PSD, DEPTH, OC and BD; TEST_CHEM+: samples with measured PSD, DEPTH, OC, BD, CACO3, PH_H2O and CEC; N: number of samples.

Preprints (www.preprints.org) | NOT PEER-REVIEWED | Posted: 28 February 2020 doi:10.20944/preprints202002.0425.v1

FIGURES

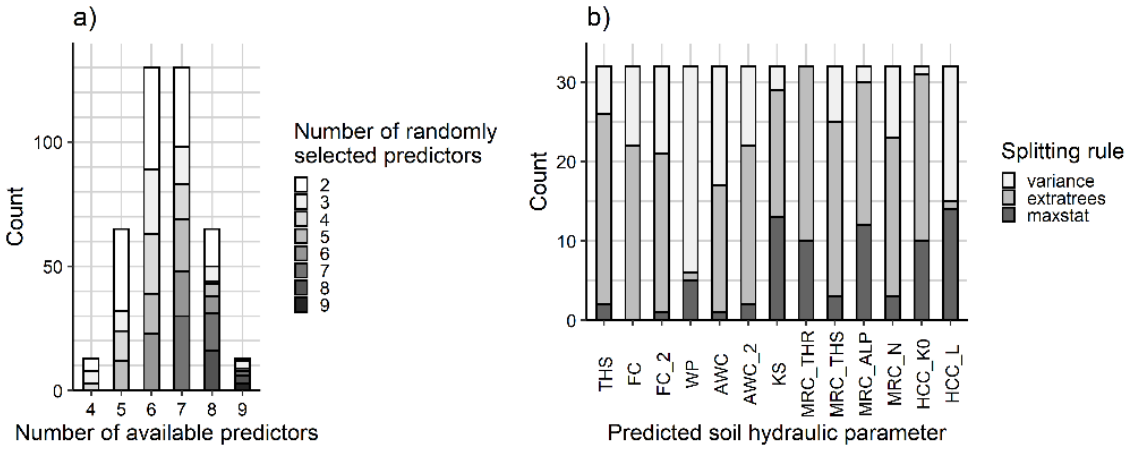

Figure 1. Results of parameter tuning of the random forest: optimization of a) the number of randomly selected predictors at each split by number of available predictors and b) splitting rule applied to build the trees in the random forest.

Preprints (www.preprints.org) | NOT PEER-REVIEWED | Posted: 28 February 2020 doi:10.20944/preprints202002.0425.v1

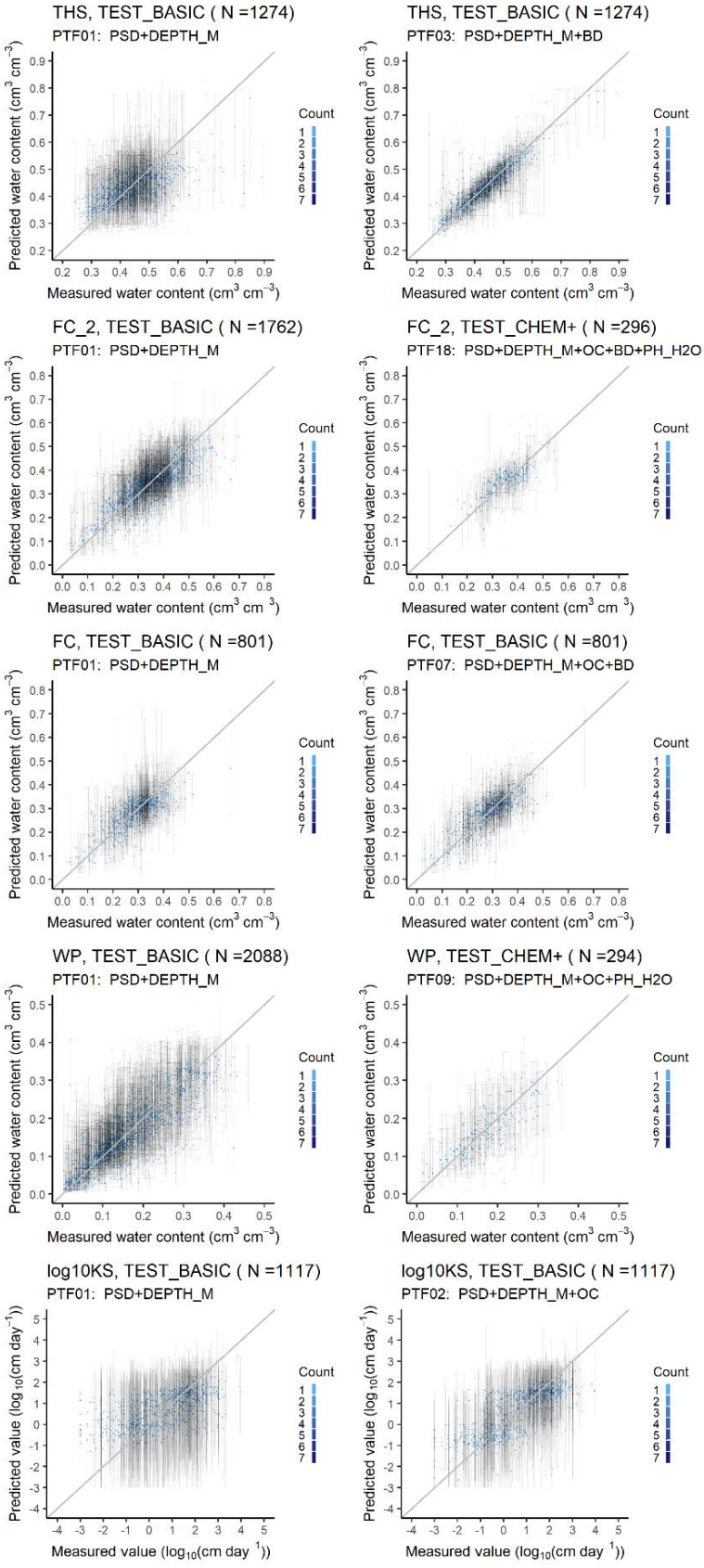

Figure 2. Scatter plot of the measured versus median predicted water retention values of the worst and best performing PTF with 90% prediction interval on test datasets. THS: saturated water content (PTF01 vs. PTF03); FC_2: water content at -100 cm matric potential head (PTF01 vs. PTF18); FC: water content at -330 cm matric potential head (PTF01 vs. PTF07); WP: water content at wilting point (PTF01 vs. PTF09); log10KS: saturated hydraulic conductivity (PTF01 vs. PTF02); PSD: particle size distribution (sand, 50–2000 µm; silt, 2–50 µm; clay, <2 µm (mass %)); DEPTH_M: mean soil depth (cm); OC: organic carbon content (mass %); BD: bulk density (g cm^{-3}); PH_H2O: pH in water (-).

Preprints (www.preprints.org) | NOT PEER-REVIEWED | Posted: 28 February 2020 doi:10.20944/preprints202002.0425.v1

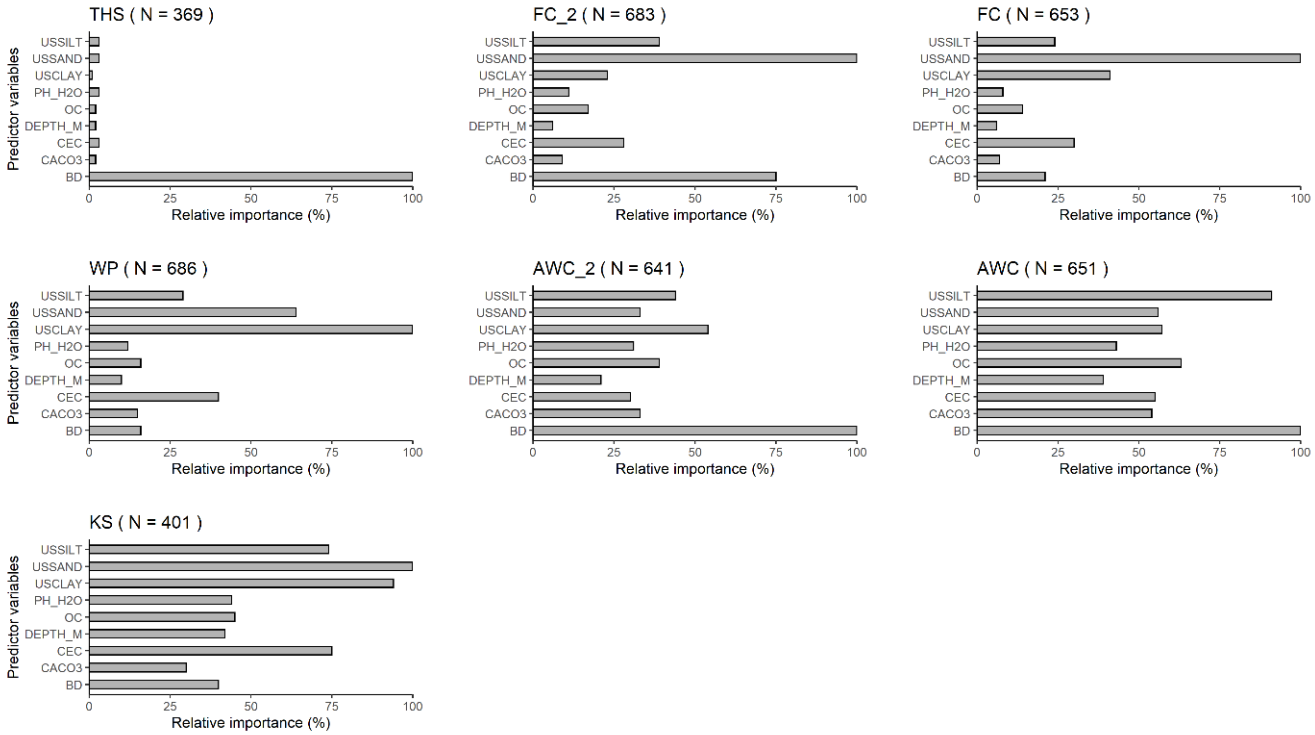

Figure 3. Variable importance computed with the random forest algorithm for the prediction of water content with PTF32 at saturation (THS), at field capacity; -100 (FC_2) and -330 (FC) matric potential head, at wilting point (WP), of the plant available water content based on FC_2 (AWC_2) and FC (AWC), and the saturated hydraulic conductivity (KS). USSILT: silt content (2–50 µm (mass %)); USSAND: sand content (50–2000 µm (mass %)); USCLAY: clay content (<2 µm (mass %)); PH_H2O: pH in water (-); OC: organic carbon content (mass %); DEPTH_M: mean soil depth (cm); OC: organic carbon content (mass %); CEC: cation exchange capacity (cmol (+) kg^{-1}); CACO3: calcium carbonate content (mass %); BD: bulk density (g cm^{-3}).

Preprints (www.preprints.org) | NOT PEER-REVIEWED | Posted: 28 February 2020 doi:10.20944/preprints202002.0425.v1

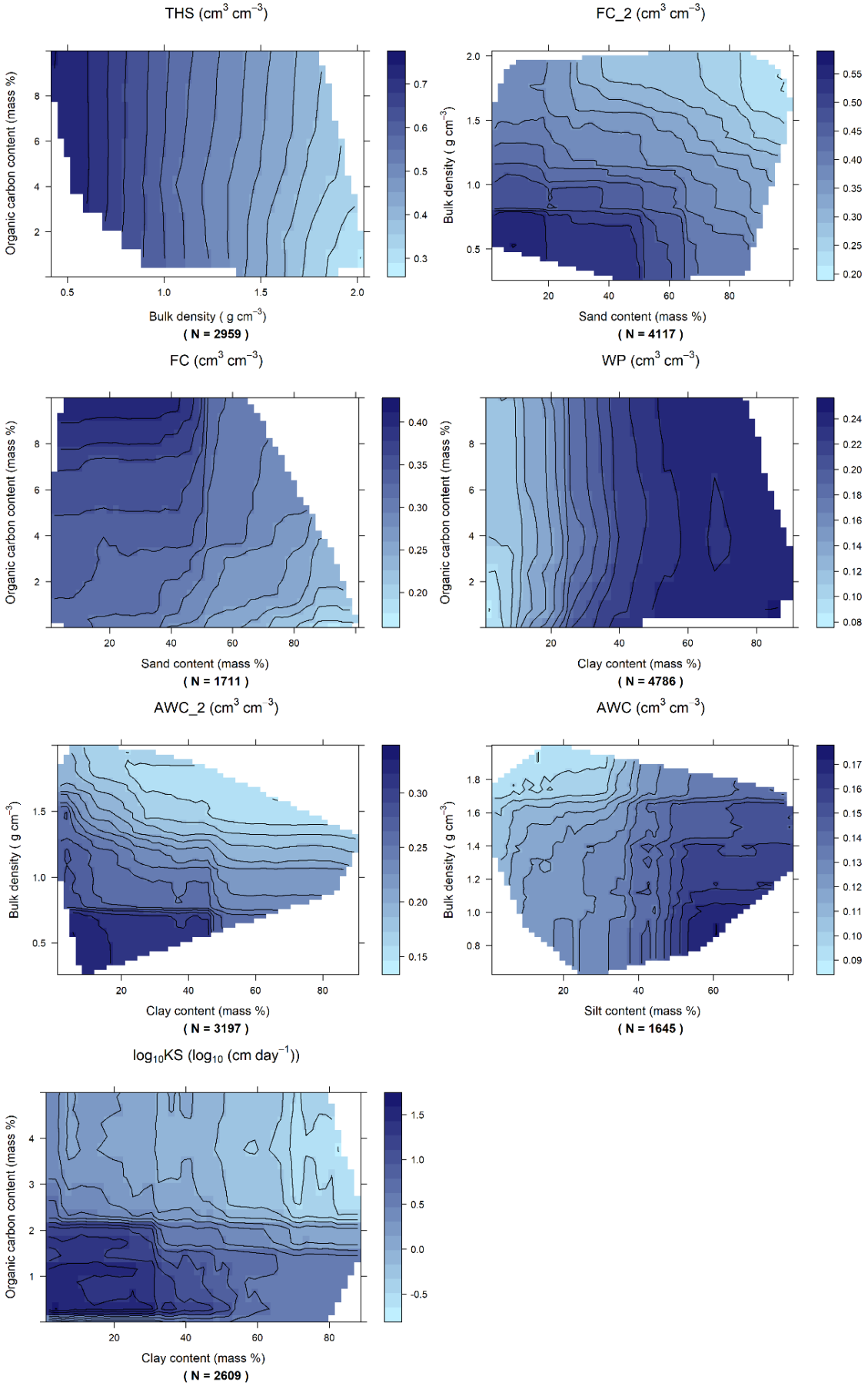

Figure 4. Partial dependence plot computed based on the random forest algorithm (PTF07) for the prediction of water content at saturation (THS), field capacity at -100 (FC_2) and -330 (FC) matric potential head, wilting point (WP), plant available water content computed with field capacity at -100 and -330 cm matric potential head (AWC_2, AWC) and saturated hydraulic conductivity (KS) for selected predictors.

Preprints (www.preprints.org) | NOT PEER-REVIEWED | Posted: 28 February 2020 doi:10.20944/preprints202002.0425.v1

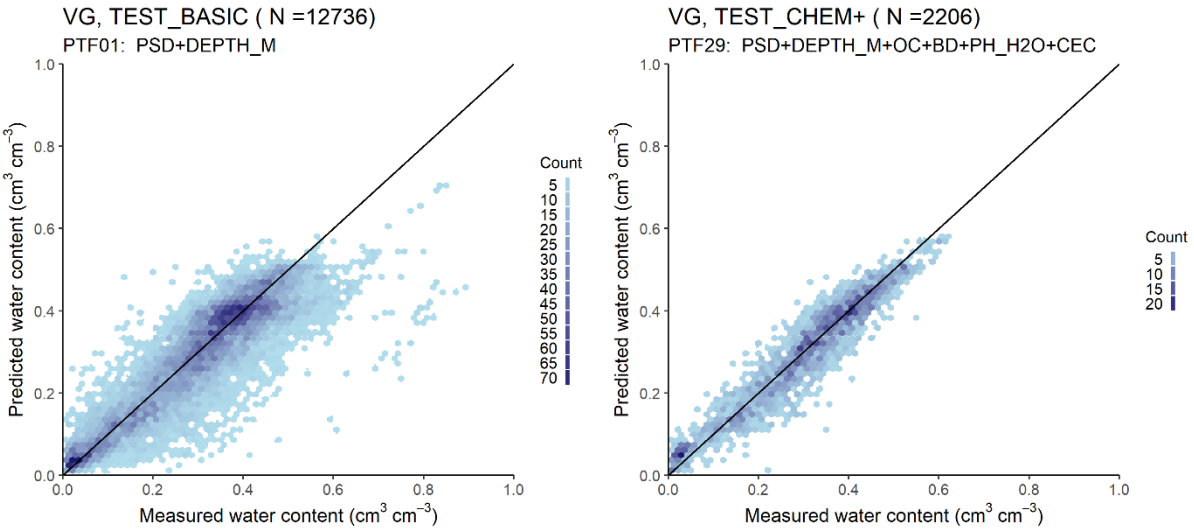

Figure 5. Scatter plot of the measured versus median predicted water retention values computed with the van Genuchten (VG) model (PTF01 vs. PTF29, i.e. the worst versus best performing PTF). PSD: particle size distribution (sand, 50–2000 µm; silt, 2–50 µm; clay, <2 µm (mass %)); DEPTH_M: mean soil depth (cm); OC: organic carbon content (mass %); BD: bulk density (g cm^{-3}); PH_H2O: pH in water (-); CEC: cation exchange capacity (cmol (+) kg^{-1}).

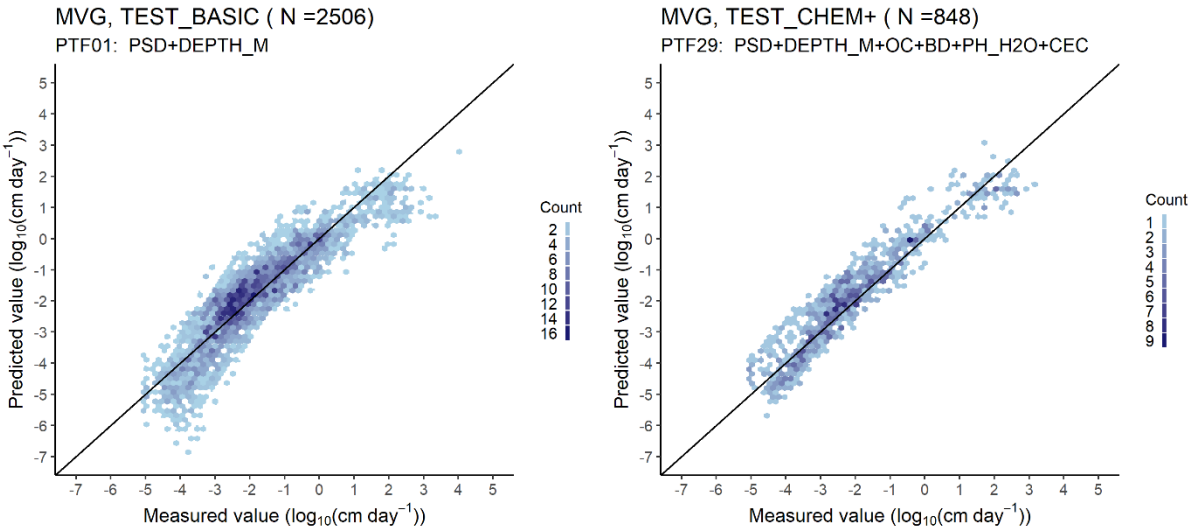

Figure 6. Scatter plot of the measured versus median predicted hydraulic conductivity values computed with the Mualem-van Genuchten (MVG) model (PTF01 vs. PTF27, i.e. the worst versus best performing PTF). PSD: particle size distribution (sand, 50–2000 µm; silt, 2–50 µm; clay, <2 µm (mass %)); DEPTH_M: mean soil depth (cm); OC: organic carbon content (mass %); BD: bulk density (g cm^{-3}); CACO3: calcium carbonate content (mass %); PH_H2O: pH in water (-).

Preprints (www.preprints.org) | NOT PEER-REVIEWED | Posted: 28 February 2020 doi:10.20944/preprints202002.0425.v1

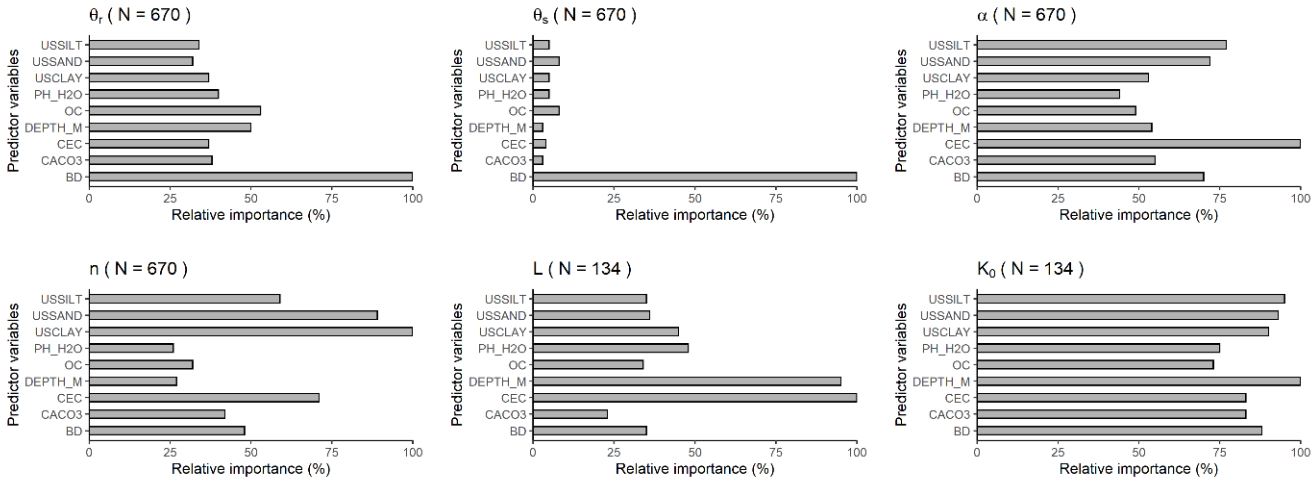

Figure 7. Variable importance computed with the random forest algorithm for the prediction of parameters of the van Genuchten and Mualem-van Genuchten model based on PTF32. θ_r: residual water content (cm³ cm^{-3}); θ_s: saturated water content (cm³ cm^{-3}); α (cm^{-1}), n (-): fitting parameters; K_0: the hydraulic conductivity acting as a matching point at saturation (cm day^{-1}); L: shape parameter related to pore tortuosity (-); USSILT: silt content (2–50 µm (mass %)); USSAND: sand content (50–2000 µm (mass %)); USCLAY: clay content,(<2 µm (mass %)); PH_H2O: pH in water (-); OC: organic carbon content (mass %); DEPTH_M: mean soil depth (cm); OC: organic carbon content (mass %); CEC: cation exchange capacity (cmol (+) kg^{-1});> CACO3: calcium carbonate content (mass %); BD: bulk density (g cm^{-3}).